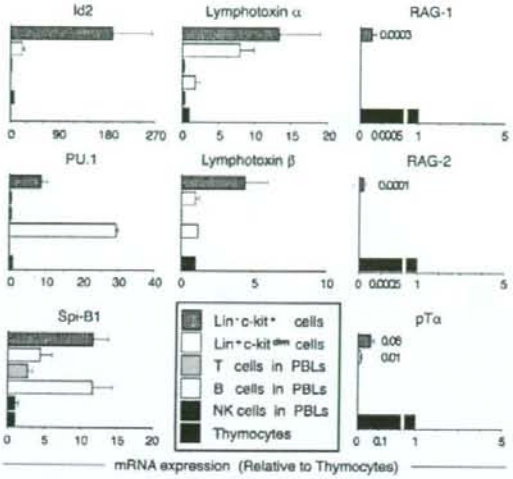

Figure 4. The lin⁻ c-kit⁺ subset has abundant mRNA for Id2, PU.1, SpiB1, and lymphotoxin α and β mRNA transcripts for each gene were quantified using real-time reverse-transcription PCR. In each sample, mRNA transcripts were normalized to those of β-actin. The expression value of each mRNA is shown as a ratio against that of thymocytes. Peripheral T, B, and NK cells were used as controls. Results are expressed as means ± SEM. The data are representative of 4 samples.

We next analyzed the lin⁺ c-kit^{dim} subset in LPMCs (Figure 3*B*). The lin⁻ c-kit^{dim} cells expressed only CD3 and CD56 among the lineage markers, and CD56⁺ cells predominated over CD3⁺ cells. The lin⁺ c-kit^{dim} subset also expressed other NK markers, IL-2Rβ and CD161, and these phenotypes corresponded to those of NKPs.[31,32] Interestingly, they expressed CD83 (Figure 3*B*), but they did not express other dendritic cell markers such as CD80, CD86, and CD209 (data not shown). It was also an intriguing finding that a fraction of these cells expressed integrin α_E, known as an IEL marker (Figure 3*B*).[33]

With the surface antigen expression patterns, the lin⁻ c-kit⁺ cells in the LPMCs were reminiscent of T/NKPs. On the other hand, the lin⁺ c-kit^{dim} subset likely may be a group of cells that already have begun differentiation into NK cells.

The lin⁻ c-kit⁺ Subset Has Abundant mRNA for Id2, PU.1, SpiB1, and Lymphotoxin

To confirm further the immature nature and differentiation potential of the lin⁻ c-kit⁺ cells, we examined the mRNA expression of several transcription factors essential for HSC differentiation. PU.1 and SpiB1 play important roles in HSC differentiation[34,35] and Id2 is essential for NK cell development.[36] The lin⁻ c-kit⁺ cells had much more abundant expression of Id2, PU.1, and SpiB1 mRNA compared with thymocytes (Figure 4). Note that mRNA of these transcription factors was decreased in the lin⁺ c-kit^{dim} cells, suggesting that they were at a later stage of differentiation than the lin⁻ c-kit⁺ population.

In addition to these transcription factors, we analyzed lymphotoxin α and β mRNA transcripts. Lymphotoxin α and β are reported to be critical for both NK cell development[37] and fulfillment of LTi functions.[38] The lin⁻ c-kit⁺ cells also had much more abundant mRNA transcripts of lymphotoxin α and β compared with thymocytes (Figure 4).

We next examined RAG-1, RAG-2, and pTα mRNA, which are essential for early T-cell differentiation. Although these transcripts were detectable in the lin⁻ c-kit⁺ cells, their expressions were far lower than that in thymocytes (Figure 4). These results indicate that the lin⁻ c-kit⁺ cells have an immature nature and the potential to differentiate into NK cells.

The lin⁻ c-kit⁺ LPMCs Are Committed to NK Cell Lineage In Vitro

Based on the results obtained so far, we assumed that the lin⁻ c-kit⁺ cells in the human adult intestine were a subset very close to T/NKPs. To confirm the differentiation capacity of the lin⁻ c-kit⁺ cells, we cultured LPMCs after depletion of both CD3⁺ and CD56⁺ cells without any exogenous stimuli. This culture method can maintain the interaction of the c-kit⁺ cells with the surrounding cells, via cell–cell contact or humoral soluble factors, which may be essential for the differentiation process. At the beginning of the culture period, we confirmed that the lin⁺ c-kit^{dim} subset was excluded completely because of CD3⁺ and CD56⁺ cell depletion (Figure 5*A*). However, surprisingly, c-kit^{dim} cells expressing lineage markers emerged and increased during the culture period (Figure 5*A* and *B*). Conversely, the lin⁻ c-kit⁻ cells gradually decreased. These lin⁺ c-kit^{dim} cells must have developed from the lin⁻ c-kit⁺ subset because the c-kit^{dim} cells did not emerge from the sorted c-kit⁻ population during 72 hours of culture (Supplementary Figure 1; supplementary material online at www.gastrojournal.org).

The c-kit⁻ cells became larger in size and had more granularity as they developed (Figure 5*C*). Most of the c-kit^{dim} cells up-regulated NK cell markers such as CD56, CD161, and IL-2Rβ, and they also expressed integrin α_E (Figure 5*C*, *D*, and *E*, Table 1). However, they did not express activated NK cell markers CD80 and CD86 (Table 1).[39] Meanwhile, very few CD3⁺ cells could be detected among the lin⁺ c-kit^{dim} populations (Figure 5*C* and *D*). Furthermore, the CD56⁺ cells in the newly emerging lin⁺ c-kit^{dim} cells contained cytotoxic granules (Figure 5*F*) and they could exert cytotoxicity against K562 cells (Figure 5*G*). They also were able to produce IFN-γ and TNF-α (Figure 5*H*). According to some previous studies, it takes up to 2 weeks for NK cell development from HSC in vitro culture.[40] Therefore, the lin⁻ c-kit⁺ subset likely included the population that already committed to NK cell lineage.

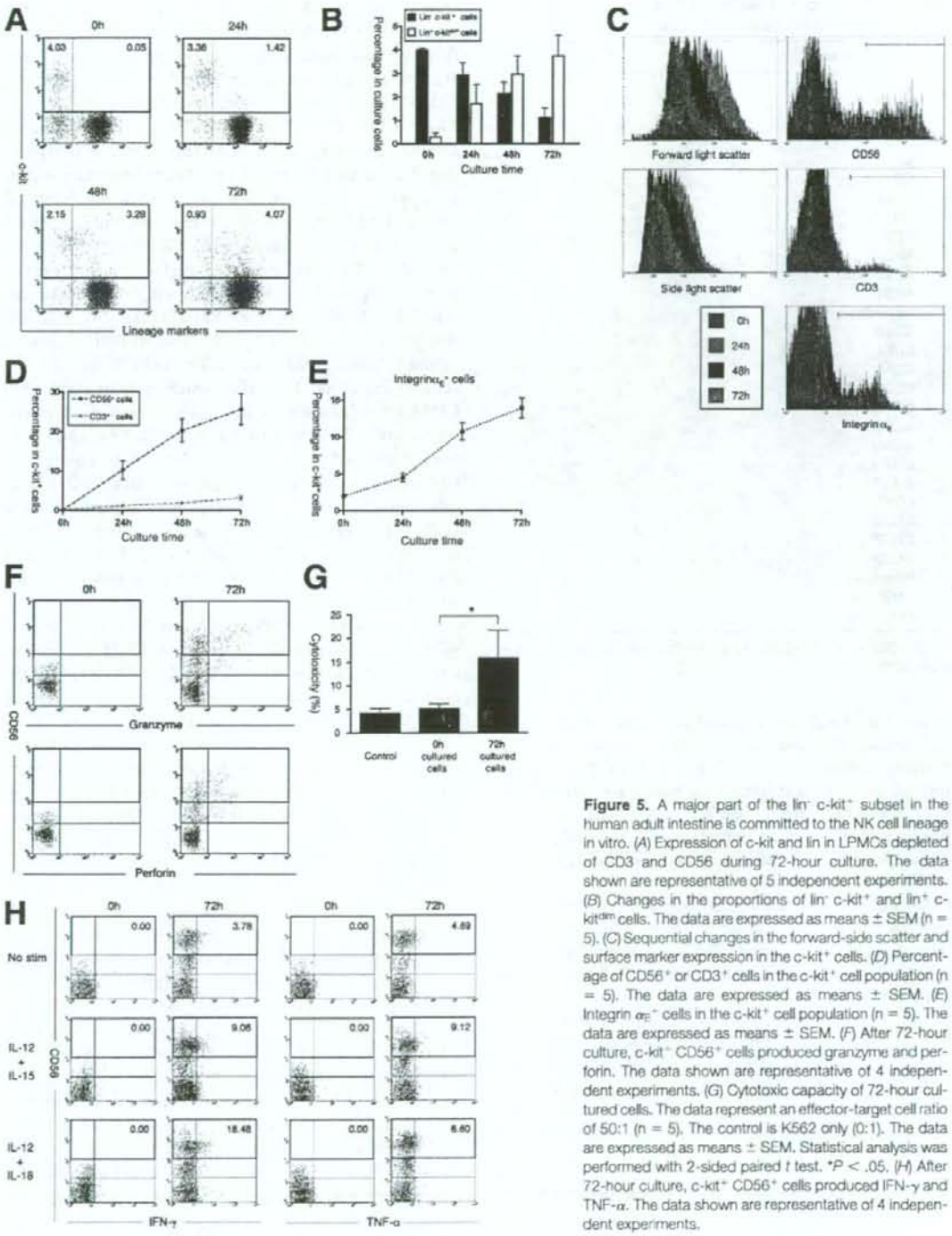

Figure 5. A major part of the lin⁻ c-kit⁺ subset in the human adult intestine is committed to the NK cell lineage in vitro. (*A*) Expression of c-kit and lin in LPMCs depleted of CD3 and CD56 during 72-hour culture. The data shown are representative of 5 independent experiments. (*B*) Changes in the proportions of lin⁻ c-kit⁺ and lin⁺ c-kit^{dim} cells. The data are expressed as means ± SEM (n = 5). (*C*) Sequential changes in the forward-side scatter and surface marker expression in the c-kit⁺ cells. (*D*) Percentage of CD56⁺ or CD3⁺ cells in the c-kit⁺ cell population (n = 5). The data are expressed as means ± SEM. (*E*) Integrin α_E⁺ cells in the c-kit⁺ cell population (n = 5). The data are expressed as means ± SEM. (*F*) After 72-hour culture, c-kit⁺ CD56⁺ cells produced granzyme and perforin. The data shown are representative of 4 independent experiments. (*G*) Cytotoxic capacity of 72-hour cultured cells. The data represent an effector-target cell ratio of 50:1 (n = 5). The control is K562 only (0:1). The data are expressed as means ± SEM. Statistical analysis was performed with 2-sided paired t test. *$P < .05$. (*H*) After 72-hour culture, c-kit⁺ CD56⁺ cells produced IFN-γ and TNF-α. The data shown are representative of 4 independent experiments.

Table 1. Phenotypes of the Newly Emerging c-kit^{dim} Cells After 72-Hour In Vitro Culture

Cell surface markers	Cultured cells (72 h)
CD34	–
CD38	+++
CD33	++
CD2	+++
CD7	++
CD11b	+
CD11c	+
CD161	+++
CD94	+
NKG2D	+
CD158a/b	–
NKB1	–
L-selectin	–
CD80	–
CD83	+
CD86	–
CD209	–
IL-2Rα	++
IL-2Rβ	++
IL-3Rα	–/+
IL-7Rα	+++
IL-18Rα	+++
CCR7	+
CXCR3	+
CXCR5	–
CX3CR1	–
Integrin α_4	+++
Integrin β_7	+
Integrin α_E	+

–, 0%–5%; –/+, 5%–10%; +, 10%–50%; ++, 50%–75%; +++, 75%–100%.

When only isolated lin$^-$ c-kit$^+$ cells were rendered to in vitro culture, they lost viability with or without exogenous human cytokines such as IL-2 and/or IL-15. Then we performed transfer experiments in which RAG-2–deficient mice received isolated human lin$^-$ c-kit$^+$ LPMCs. Very surprisingly, 3 weeks after transplantation we could detect human lin$^-$ c-kit$^+$ cells exclusively in murine LPMCs but not in IELs or splenic lymphocytes (Figure 6*A*). The absence of CD56 expression indicated that they did not differentiate into NK cells in murine intestine. However, human CD56$^+$ cells emerged when murine LPMCs containing human lin$^-$ c-kit$^+$ cells were cultured with exogenous IL-2 and/or IL-15 (Figure 6*B*).

These results suggested that a large proportion of human LP lin$^-$ c-kit$^+$ cells were the NK cell precursors. Given that newly emerging lin$^+$ c-kit^{dim} cells from lin$^-$ c-kit$^+$ subtype shared a very similar phenotype with the lin$^+$ c-kit^{dim} cells that actually reside in human LPMCs (Figure 3B and Table 1), this differentiation process may actually occur in the human intestine.

LPMCs and IELs Contain Functional NK Cells

The results thus far have indicated that the lin$^-$ c-kit$^+$ cells in the intestine have the potential to differentiate into NK cells. There have been only a few reports on NK cells in the human intestine,[41,42] therefore, we examined CD56 expression on LPMCs and IELs. It revealed that a considerable number of CD3$^-$ CD56$^+$ cells certainly exist in LPMCs (Figure 7*A*). These CD3$^-$ CD56$^+$ cells, which are referred to as LPNKs, were larger and had more granular morphology than lamina propria T cells (Supplementary Figure 2; supplementary material online at www.gastrojournal.org). CD3$^-$ CD56$^+$ cells also were found in IELs, which are referred to as intraepithelial NK cells (IENKs) (Figure 7*A*).[42] We next compared surface marker expression among the lin$^-$ c-kit$^+$, lin$^+$ c-kit^{dim}, and intestinal NK cells (LPNKs and IENKs) (Figure 7*B*). NK cell markers such as CD94, CD161, and NKG2D increased in the following order: lin$^-$ c-kit$^+$ cells < lin$^+$ c-kit^{dim} cells < intestinal NK cells, which is consistent with CD56 up-regulation on lin$^+$ c-kit^{dim} cells. Conversely, immature cell markers such as c-kit, IL-7Rα, and CD33 were decreased in the same order. These changes in surface marker expression also were observed during differentiation of lin$^-$ c-kit$^+$ cells into lin$^+$ c-kit^{dim} cells (Table 1). Taken together, these results would support the hypothesis that lin$^-$ c-kit$^+$ cells differentiate into intestinal NK cells via lin$^+$ c-kit^{dim} cells, possibly at the site of the intestine.

It is known that PBNK cells can be divided into 2 subsets according to the intensity of CD56 expression: CD56^{dim} and CD56^{bright} NK cells.[43,44] Although CD56 expression on the intestinal NK cells was not as high as on CD56^{bright} NK cells, the intestinal NK cells were reminiscent of CD56^{bright} NK cells owing to the lack of CD16, CX3CR1, and killer cell inhibitory receptor (CD158a/b, NKB1) expression (Figure 7*B*).[45,46] Moreover, both the intestinal NK cells and the peripheral CD56^{bright} NK cells expressed CD33, whereas the peripheral CD56^{dim} NK cells did not (Figure 7*B*).

To confirm that the intestinal NK cells harbor NK functions, cytotoxic molecules were examined. Both LPNKs and IENKs contained granzyme and perforin; and they were equipped with cytotoxic function, although the activity was weaker than that in peripheral CD56^{dim} NK cells (Figure 7*C* and *D*). Both LPNKs and IENKs also produced IFN-γ and TNF-α at a level comparable with peripheral CD56^{bright} NK cells (Figure 7*E–H*). With these phenotypes (ie, lower expression of granzyme and perforin and higher IFN-γ and TNF-α production), intestinal NK cells are reminiscent of peripheral CD56^{bright} NK cells. However, they clearly were discriminated from peripheral CD56^{bright} NK cells in terms of CD83 and integrin α_E expression (Figure 7*B*). These unique characteristics of intestinal NK cells may support the idea that they may have an original in situ differentiation system independent from PBNKs.

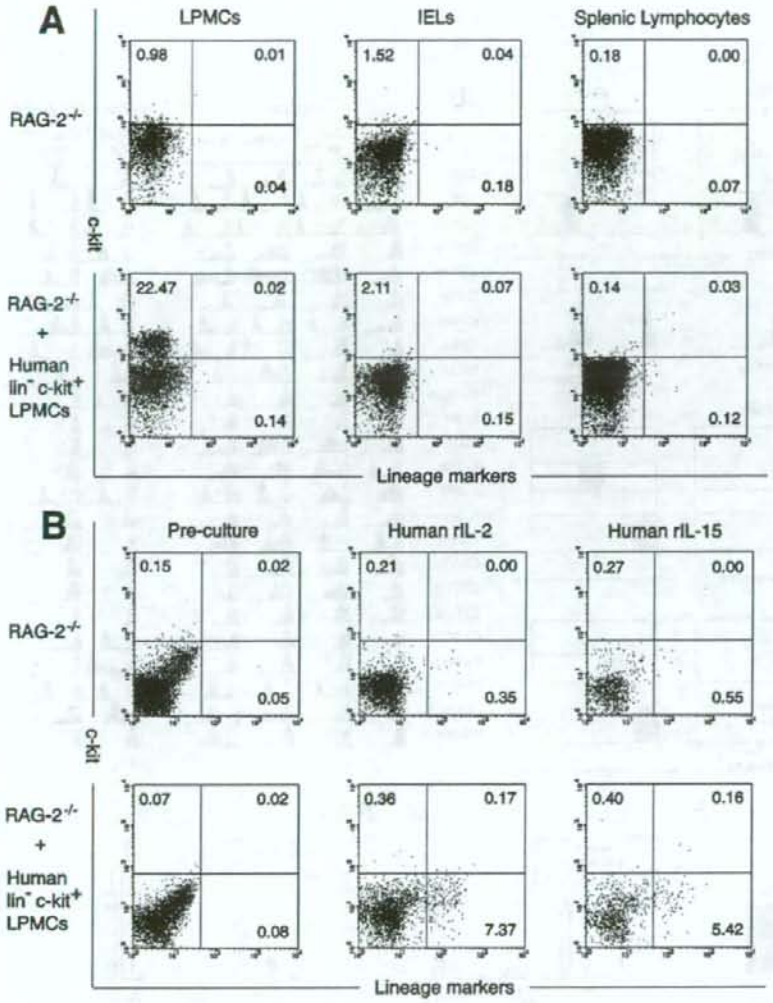

Figure 6. Human lin⁻ c-kit⁺ LPMCs after the transfer into recipient mice could differentiate into NK cells. (*A*) LPMCs, IELs, and splenic lymphocytes isolated from the RAG$^{-/-}$ mice transplanted with human lin⁻ c-kit⁺ LPMCs were stained by lineage markers and CD117 monoclonal antibody and were analyzed by fluorescence-activated cell sorter. The data shown are representative of 2 independent experiments. (*B*) Isolated LPMCs were cultured with human recombinant IL-2 (rIL-2) or rIL-15 for 7 days. The cultured cells were analyzed for expression of human CD3 and CD56. The data shown are representative of 2 independent experiments.

Intestinal NK Cells Are Increased in CD, Reflecting Accelerated Differentiation of lin⁻ c-kit⁺ Cells Into NK Cells

The involvement of NK cells in intestinal inflammation has not been well documented. Therefore, we examined intestinal NK cells in inflammatory bowel disease, a chronic inflammatory condition that consists of 2 major forms: CD and UC.[47] Flow cytometry revealed that both LPNKs and IENKs were increased in the samples from CD but not from UC patients, compared with

Figure 7. Analysis of surface antigen expression and function of intestinal NK cells. (*A*) LPMCs, IELs, and PBLs were stained for CD3 and CD56. CD3⁻ CD56⁺ cells were examined further for c-kit expression. (*B*) Expression of various surface markers, including NK cell markers, was compared among lin⁻ c-kit⁺ and lin⁺ c-kit^{dim} cells, LPNKs, IENKs, and PBNKs. The data shown are representative of more than 4 cases for each surface marker. (*C*) Production of granzyme, perforin from LPNKs, IENKs, and PBNKs were determined with intracellular staining. The data shown are representative of 4 independent experiments. (*D*) Cytotoxicity of freshly isolated LPNKs (n = 5) and PBNKs (n = 4). Effector-target ratio was 10:1. The data were expressed as means ± SEM. (*E*) IFN-γ and (*F*) TNF-α production from LPNKs (n = 5) and PBNKs (n = 4) after 72-hour culture with indicated cytokines. The data were expressed as means ± SEM. (*G*) IFN-γ or (*H*) TNF-α production in LPNKs, IENKs, and PBNKs after 8 hours of cytokine stimulation were detected using the Cytokine Secretion Assay Cell Detection Kit (Miltenyi Biotec). The data shown are representative of 4 independent experiments.

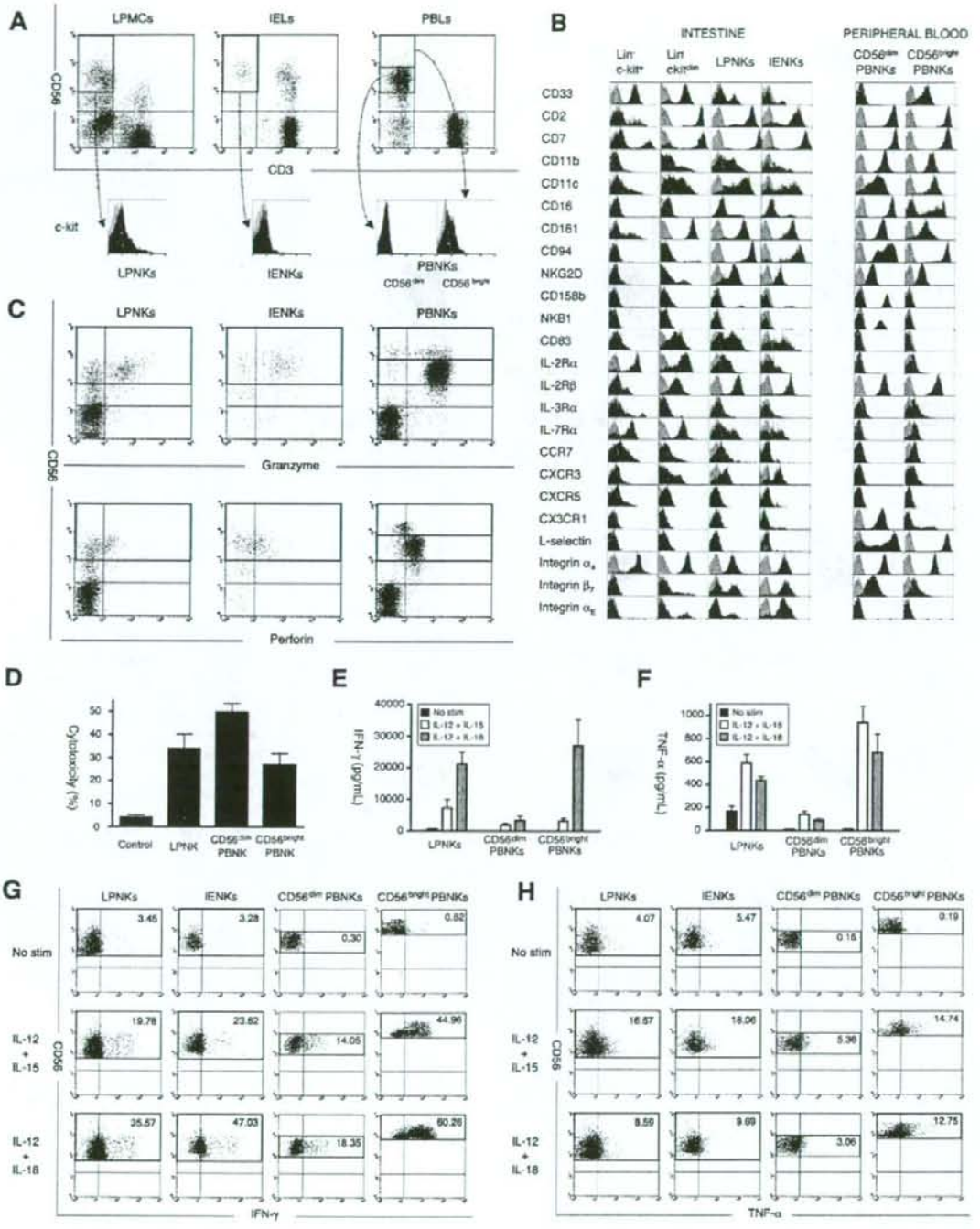
A
LPMCs
IELs
PBLs
CD56
CD3
c-kit
LPNKs
IENKs
PBNKs
CD56dim CD56bright
B
INTESTINE
PERIPHERAL BLOOD
Lin- c-kit+
Lin- ckitdim
LPNKs
IENKs
CD56dim PBNKs
CD56bright PBNKs
CD33
CD2
CD7
CD11b
CD11c
CD16
CD161
CD94
NKG2D
CD158b
NKB1
CD83
IL-2Rα
IL-2Rβ
IL-3Rα
IL-7Rα
CCR7
CXCR3
CXCR5
CX3CR1
L-selectin
Integrin αe
Integrin βp
Integrin αE
C
LPNKs
IENKs
PBNKs
CD56
Granzyme
Perforin
D
Cytotoxicity (%)
Control
LPNK
CD56dim PBNK
CD56bright PBNK
E
IFN-γ (pg/mL)
No stim
IL-12 + IL-15
IL-12 + IL-18
LPNKs
CD56dim PBNKs
CD56bright PBNKs
F
TNF-α (pg/mL)
No stim
IL-12 + IL-15
IL-12 + IL-18
LPNKs
CD56dim PBNKs
CD56bright PBNKs
G
LPNKs
IENKs
CD56dim PBNKs
CD56bright PBNKs
No stim
IL-12 + IL-15
IL-12 + IL-18
CD56
IFN-γ
3.45
3.28
0.30
0.92
19.78
23.62
14.05
44.96
35.57
47.03
18.35
60.26
H
LPNKs
IENKs
CD56dim PBNKs
CD56bright PBNKs
No stim
IL-12 + IL-15
IL-12 + IL-18
CD56
TNF-α
4.07
5.47
0.15
0.19
16.57
18.06
5.36
14.74
8.59
9.69
3.06
12.75

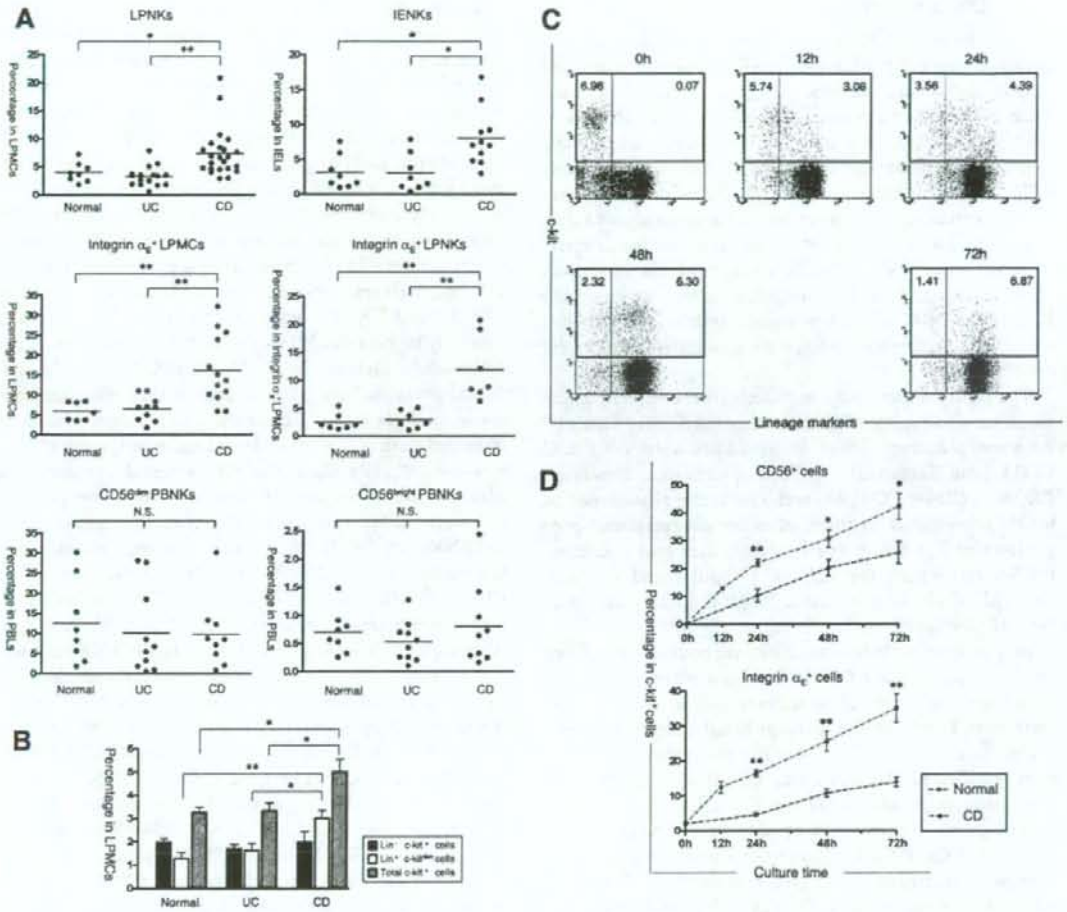

Figure 8. The c-kit^{dim} cells, LPNKs, and IENKs are increased in CD. (*A*) Percentage of NK cells among LPMCs (normal, n = 10; UC, n = 17; CD, n = 23) or IELs (normal, n = 8; UC, n = 8; CD, n = 11) (upper panels). Percentage of integrin $\alpha_E\beta_7^+$ cells among LPMCs (normal, n = 7; UC, n = 10; CD, n = 13) or LPNKs (normal, n = 7; UC, n = 7; CD, n = 7) (middle panels). Percentage of CD56^{dim} CD16$^+$ and CD56^{bright} CD16$^-$ NK cells among PBLs (normal, n = 8; UC, n = 10; CD, n = 9) (bottom panels). Statistical analysis was performed with the Kruskal–Wallis 1-way analysis of variance, and the Bonferroni–Dunn test for multiple comparisons. $^*P < .05$, $^{**}P < .01$. (*B*) Percentage of total c-kit$^+$, lin$^-$ c-kit$^+$, or lin$^+$ c-kit^{dim} cells among LPMCs (normal, n = 10; UC, n = 11; CD, n = 15). Results are expressed as means ± SEM. Statistical analysis was performed with the Kruskal–Wallis 1-way analysis of variance, and the Bonferroni–Dunn test for multiple comparisons. $^*P < .05$, $^{**}P < .01$. (*C*) LPMCs depleted of CD3 and CD56, obtained from CD patients, were cultured for 72 hours and analyzed for expression of c-kit and lin. The data shown are representative of 7 independent experiments. (*D*) The line graph shows the time–course changes for CD56+ or integrin α_E^+ cells in c-kit$^+$ LPMCs from normal controls (n = 5) or CD patients (n = 7). The data are expressed as means ± SEM for the percentage of CD56$^+$ or integrin α_E^+ cells among the c-kit$^+$ cells. Statistical analysis was performed with a 2-sided Mann–Whitney *U* test. $^*P < .05$, $^{**}P < .01$.

normal controls (Figure 8*A*). In contrast, the frequency of NK cells, both for CD56^{dim} and CD56^{bright}, was similar in peripheral blood among the 3 groups (Figure 8*A*). Furthermore, although lin$^-$ c-kit$^+$ cells existed with similar frequency, the lin$^+$ c-kit^{dim} cells were increased significantly in CD compared with UC or normal controls (Figure 8*B*). Then we repeated the in vitro culture experiments shown in Figure 5 and found that more lin$^+$ c-kit^{dim} cells were detected in CD samples at each time point (Figure 8*C*), and the majority of these cells expressed CD56 and integrin α_E (Figure 8*D*). Taken together, the increase of LPNKs and IENKs in CD patients could have been owing to accelerated differentiation from lin$^-$ c-kit$^+$ cells. Given that the intestinal NK cells can strongly produce IFN-γ and TNF-α, which is a key cytokine in the pathogenesis of CD, these increased intestinal NK cells may play a pathogenic role in chronic inflammation in CD.

Discussion

The sites of NK cell development in adults are understood poorly.[40,48] Although T/NKPs have been identified only in fetal tissues, the bone marrow is presumed to be the main site of NK cell generation in adults.[40,48] In this study, we have shown that lin$^-$ c-kit$^+$ cells in human adult intestine could differentiate into c-kit^{dim} cells, which express CD56 during in vitro culture, suggesting that these cells are NK cell precursors. Moreover, further analysis showed that in vitro differentiated c-kit^{dim} CD56$^+$ cells seemed to correspond to c-kit^{dim} CD56$^+$ cells actually present in human adult intestine. Combined together, adult intestine may have unique NK cell differentiation system in which lin$^-$ c-kit$^+$ NK precursors undergo in situ differentiation via c-kit^{dim} cells.

The newly discovered c-kit$^+$ cells in the human adult intestine also express CD34, another marker for HSCs or immune precursor cells.[17,28] In addition to c-kit and CD34, the intestinal immune precursors expressed CD38^{dim}, CD44, CD45RA, and Thy-1, the phenotypes of which correspond to those of common lymphoid progenitors or T/NKPs.[49] Furthermore, they had abundant mRNA transcripts for Id2, PU.1, SpiB1, and lymphotoxin, all of which are essential for HSC differentiation or NK cell development.

In the murine intestine, c-kit–expressing cells form small clusters named CP.[8] It has been reported that CP cells have the potential to differentiate mainly into extrathymic T cells in the intraepithelial space.[10] Interestingly, the intestinal c-kit$^+$ immune precursor cell expression level of RAG mRNA was very low, and the RAG expression level was similar to CP cells, which was reported previously by Oida et al.[50] Recent studies have shown that CD3$^-$ CD7$^+$ cells in the human fetal intestine express pTα mRNA[13] and give rise to CD3$^+$ T cells in vitro and in vivo, using SCID mice with engrafted human fetal intestine.[14] The intestinal c-kit$^+$ immune precursor cells are also CD3$^-$ CD7$^+$ and express RAG-1, RAG-2, and pTα mRNA. These results imply that the immune precursor cells in adult intestine include a subset similar or identical to the CD3$^-$ CD7$^+$ cells in the fetal intestine and they may differentiate into T cells in unusual environment, such as lymphopenia. However, in that they do not form aggregates and are much more committed to NK cells rather than T cells, they should be distinguished from the murine CP cells that differentiate into intraepithelial T cells. On the other hand, a recent study showed that c-kit$^+$ cells in CP represent LTi in adult mice, which organize isolated lymphoid follicles.[12] Furthermore, because LTi and T/NKPs have similar expression patterns of surface antigens and transcription factors,[51,52] they are considered to be subsets that are related closely to each other. Given that intestinal immune precursor cells also are similar to LTi in terms of surface antigen expression and transcriptional profile, it is possible that they contain an adult LTi subset.

Little information is available about intestinal NK cells. An earlier article reported on lymphokine activated killer activity in human LPMCs,[53] although they failed to identify NK cells in LPMCs, possibly because of the lack of suitable NK cell markers at that time. Some recent reports showed that human LPMCs and IELs contain NK cells capable of killing tumor cells and producing several cytokines, such as IFN-γ and TNF-α.[41,43] In this study, we intensively examined the intestinal NK cells to verify the hypothesis that they develop in situ from the immune precursor cells in intestinal lamina propria. In terms of NK cell markers, expression of CD56, as well as CD94, CD161, and NKG2D, was lowest in the c-kit$^+$ cells, and inversely highest in LPNKs/IENKs. In contrast, immature cell markers such as c-kit, IL-7Rα, and CD33 were highest in the intestinal immune precursor cells. Furthermore, these changes in surface marker expression also were observed during in vitro differentiation of lin$^-$ c-kit$^+$ cells into c-kit^{dim} cells. Collectively, these results support the idea that intestinal immune precursor cells can give rise to intestinal NK cells via c-kit^{dim} NKP-like cells.

PBNKs can be classified into 2 subsets. One subset is the conventional CD56^{dim} NK cells and the other is the CD56^{bright} NK cells.[43,44] Absence of CD16 expression is also a characteristic feature of the CD56^{bright} NK cells. Although CD56 expression of the intestinal NK cells was not as high as the peripheral CD56^{bright} NK cells, absence of CD16 expression indicates a similarity between the intestinal NK cells and the peripheral CD56^{bright} NK cells. In addition, we found that both the intestinal NK cells, especially LPNKs, and peripheral CD56^{bright} NK cells expressed CD33. Although CD33 is a myeloid lineage marker, it is reported that CD33$^+$ CD34$^+$ HSCs can give rise to CD16$^-$ NK cells in vitro.[54] Given that most intestinal immune precursor cells express CD33, and that intestinal NK cells are CD33$^+$ CD16$^-$, it is reasonable to assume that the intestinal NK cells may originate from the immune precursor cells. Furthermore, CD33 is reported to be expressed on CD56^{bright} NK cells in umbilical cord blood[55] and on T/NKPs in the fetal thymus.[29] Although the origin of CD56^{bright} NK cells still is controversial, it recently was reported that the peripheral CD56^{bright} NK cells differentiate in the lymph nodes, unlike conventional CD56^{dim} NK cells.[56] CD33$^+$ CD16$^-$ may be a phenotype that characterizes NK cells developing outside the bone marrow, such as lymph nodes, the thymus, and maybe the intestine.

The pathophysiologic contribution of intestinal NK cells to inflammatory bowel disease has yet to be elucidated. An interesting recent report suggested that the intestinal NK cells maintain homeostasis of intestinal mucosal immune system in mice. However, their roles have not been resolved in human beings.[57] We found that the differentiation of the intestinal immune precursor cells into NK cells was accelerated in CD, resulting in an increase in the number of intestinal NK cells in CD

compared with UC or normal controls. According to the previous report, CD56^{bright} NK cells also are enriched at inflammatory sites, such as arthritis, infectious pleuritis, and bacterial peritonitis.[58] CD is regarded as a typical T helper type 1 response (Th1) disease driven by excessive IFN-γ production from dysregulated CD4 T cells infiltrating the inflamed tissue. However, given that NK cells constitute a considerable proportion of LPMCs or IELs (about 8%) and can highly produce IFN-γ, intestinal NK cells may contribute to the pathogenesis of CD. Overexpression of IFN-γ in CD may modulate intestinal NK cell differentiation because it was reported that this cytokine accelerated differentiation of human HSCs.[59]

In summary, we have identified c-kit$^+$ immune precursor cells in the human adult intestine for the first time. We also have shown that these cells are committed mainly to the NK cell lineage. Because this intestinal NK cell differentiation system may contribute to the pathophysiology of CD, further clarification of the role of intestinal NK cells will help to better understand the gut immune system and may lead to new therapeutic strategies against CD.

Appendix

Supplementary data

Supplementary data associated with this article can be found, in the online version, at doi:10.1053/j.gastro.2007.05.017.

References

1. Akashi K, Traver D, Miyamoto T, Weissman IL. A clonogenic common myeloid progenitor that gives rise to all myeloid lineages. Nature 2000;404:193–197.
2. Kondo M, Weissman IL, Akashi K. Identification of clonogenic common lymphoid progenitors in mouse bone marrow. Cell 1997; 91:661–672.
3. Rodewald HR, Moingeon P, Lucich JL, Dosiou C, Lopez P, Reinherz EL. A population of early fetal thymocytes expressing Fc gamma RII/III contains precursors of T lymphocytes and natural killer cells. Cell 1992;69:139–150.
4. Carlyle JR, Michie AM, Furlonger C, Nakano T, Lenardo MJ, Paige CJ, Zuniga-Pflucker JC. Identification of a novel developmental stage marking lineage commitment of progenitor thymocytes. J Exp Med 1997;186:173–182.
5. Ikawa T, Kawamoto H, Fujimoto S, Katsura Y. Commitment of common T/Natural killer (NK) progenitors to unipotent T and NK progenitors in the murine fetal thymus revealed by a single progenitor assay. J Exp Med 1999;190:1617–1626.
6. Yoshida H, Honda K, Shinkura R, Adachi S, Nishikawa S, Maki K, Ikuta K, Nishikawa SI. IL-7 receptor alpha+ CD3(-) cells in the embryonic intestine induces the organizing center of Peyer's patches. Int Immunol 1999;11:643–655.
7. Finke D, Acha-Orbea H, Mattis A, Lipp M, Kraehenbuhl J. CD4+CD3- cells induce Peyer's patch development: role of alpha4beta1 integrin activation by CXCR5. Immunity 2002;17:363–373.
8. Kanamori Y, Ishimaru K, Nanno M, Maki K, Ikuta K, Nariuchi H, Ishikawa H. Identification of novel lymphoid tissues in murine intestinal mucosa where clusters of c-kit+ IL-7R+ Thy1+ lympho-hemopoietic progenitors develop. J Exp Med 1996;184:1449–1459.
9. Yoshida H, Naito A, Inoue J, Satoh M, Santee-Cooper SM, Ware CF, Togawa A, Nishikawa S, Nishikawa S. Different cytokines induce surface lymphotoxin-alphabeta on IL-7 receptor-alpha cells that differentially engender lymph nodes and Peyer's patches. Immunity 2002;17:823–833.
10. Saito H, Kanamori Y, Takemori T, Nariuchi H, Kubota E, Takahashi-Iwanaga H, Iwanaga T, Ishikawa H. Generation of intestinal T cells from progenitors residing in gut cryptopatches. Science 1998;280:275–278.
11. Suzuki K, Oida T, Hamada H, Hitotsumatsu O, Watanabe M, Hibi T, Yamamoto H, Kubota E, Kaminogawa S, Ishikawa H. Gut cryptopatches: direct evidence of extrathymic anatomical sites for intestinal T lymphopoiesis. Immunity 2000;13:691–702.
12. Eberl G, Littman DR. Thymic origin of intestinal alphabeta T cells revealed by fate mapping of RORgammat+ cells. Science 2004; 305:248–251.
13. Howie D, Spencer J, DeLord D, Pitzalis C, Wathen NC, Dogan A, Akbar A, MacDonald TT. Extrathymic T cell differentiation in the human intestine early in life. J Immunol 1998;161:5862–5872.
14. Gunther U, Holloway JA, Gordon JN, Knight A, Chance V, Hanley NA, Wilson DI, French R, Spencer J, Steer H, Anderson G, MacDonald TT. Phenotypic characterization of CD3-7+ cells in developing human intestine and an analysis of their ability to differentiate into T cells. J Immunol 2005;174:5414–5422.
15. Williams AM, Bland PW, Phillips AC, Turner S, Brooklyn T, Shaya G, Spicer RD, Probert CS. Intestinal alpha beta T cells differentiate and rearrange antigen receptor genes in situ in the human infant. J Immunol 2004;173:7190–7199.
16. Bas A, Hammarstrom SG, Hammarstrom ML. Extrathymic TCR gene rearrangement in human small intestine: identification of new splice forms of recombination activating gene-1 mRNA with selective tissue expression. J Immunol 2003;171:3359–3371.
17. Ashman LK, Cambareri AC, To LB, Levinsky RJ, Juttner CA. Expression of the YB5.B8 antigen (c-kit proto-oncogene product) in normal human bone marrow. Blood 1991;78:30–37.
18. Res P, Martinez-Caceres E, Cristina Jaleco A, Staal F, Noteboom E, Weijer K, Spits H. CD34+CD38dim cells in the human thymus can differentiate into T, natural killer, and dendritic cells but are distinct from pluripotent stem cells. Blood 1996;87:5196–5206.
19. Sanchez MJ, Spits H, Lanier LL, Phillips JH. Human natural killer cell committed thymocytes and their relation to the T cell lineage. J Exp Med 1993;178:1857–1866.
20. Lennard-Jones JE. Classification of inflammatory bowel disease. Scand J Gastroenterol Suppl 1989;170:2–6, 16–19.
21. Gower-Rousseau C, Salomez JL, Dupas JL, Marti R, Nuttens MC, Votte A, Lemahieu M, Lemaire B, Colombel JF, Cortot A. Incidence of inflammatory bowel disease in northern France (1988–1990). Gut 1994;35:1433–1438.
22. Bandeira A, Mota-Santos T, Itohara S, Degermann S, Heusser C, Tonegawa S, Coutinho A. Localization of gamma/delta T cells to the intestinal epithelium is independent of normal microbial colonization. J Exp Med 1990;172:239–244.
23. Ishikawa H, Li Y, Abeliovich A, Yamamoto S, Kaufmann SH, Tonegawa S. Cytotoxic and interferon gamma-producing activities of gamma delta T cells in the mouse intestinal epithelium are strain dependent. Proc Natl Acad Sci U S A 1993;90:8204–8208.
24. Eldridge JH, Kiyono H, Michalek SM, McGhee JR. Evidence for a mature B cell subpopulation in Peyer's patches of young adult xid mice. J Exp Med 1983;157:789–794.
25. Chang L, Gusewitch GA, Chritton DB, Folz JC, Lebeck LK, Nehlsen-Cannarella SL. Rapid flow cytometric assay for the assessment of natural killer cell activity. J Immunol Methods 1993;166:45–54.
26. Horie K, Fujita J, Takakura K, Kanzaki H, Suginami H, Iwai M, Nakayama H, Mori T. The expression of c-kit protein in human adult and fetal tissues. Hum Reprod 1993;8:1955–1962.
27. Feyerabend TB, Hausser H, Tietz A, Blum C, Hellman L, Straus AH, Takahashi HK, Morgan ES, Dvorak AM, Fehling HJ, Rodewald HR. Loss of histochemical identity in mast cells lacking carboxypeptidase A. Mol Cell Biol 2005;25:6199–6210.

28. Civin CI, Strauss LC, Brovall C, Fackler MJ, Schwartz JF, Shaper JH. Antigenic analysis of hematopoiesis. III. A hematopoietic progenitor cell surface antigen defined by a monoclonal antibody raised against KG-1a cells. J Immunol 1984;133:157–165.
29. Sanchez MJ, Muench MO, Roncarolo MG, Lanier LL, Phillips JH. Identification of a common T/natural killer cell progenitor in human fetal thymus. J Exp Med 1994;180:569–576.
30. Peiper SC, Ashmun RA, Look AT. Molecular cloning, expression, and chromosomal localization of a human gene encoding the CD33 myeloid differentiation antigen. Blood 1988;72:314–321.
31. Miller JS, Alley KA, McGlave P. Differentiation of natural killer (NK) cells from human primitive marrow progenitors in a stroma-based long-term culture system: identification of a CD34+7+ NK progenitor. Blood 1994;83:2594–2601.
32. Kim S, Iizuka K, Kang HS, Dokun A, French AR, Greco S, Yokoyama WM. In vivo developmental stages in murine natural killer cell maturation. Nat Immunol 2002;3:523–528.
33. Cepek KL, Parker CM, Madara JL, Brenner MB. Integrin alpha E beta 7 mediates adhesion of T lymphocytes to epithelial cells. J Immunol 1993;150:3459–3470.
34. Anderson MK, Hernandez-Hoyos G, Diamond RA, Rothenberg EV. Precise developmental regulation of Ets family transcription factors during specification and commitment to the T cell lineage. Development 1999;126:3131–3148.
35. Scott EW, Simon MC, Anastasi J, Singh H. Requirement of transcription factor PU.1 in the development of multiple hematopoietic lineages. Science 1994;265:1573–1577.
36. Yokota Y, Mansouri A, Mori S, Sugawara S, Adachi S, Nishikawa S, Gruss P. Development of peripheral lymphoid organs and natural killer cells depends on the helix-loop-helix inhibitor Id2. Nature 1999;397:702–706.
37. Iizuka K, Chaplin DD, Wang Y, Wu Q, Pegg LE, Yokoyama WM, Fu YX. Requirement for membrane lymphotoxin in natural killer cell development. Proc Natl Acad Sci U S A 1999;96:6336–6340.
38. Alimzhanov MB, Kuprash DV, Kosco-Vilbois MH, Luz A, Turetskaya RL, Tarakhovsky A, Rajewsky K, Nedospasov SA, Pfeffer K. Abnormal development of secondary lymphoid tissues in lymphotoxin beta-deficient mice. Proc Natl Acad Sci U S A 1997;94:9302–9307.
39. Hanna J, Gonen-Gross T, Fitchett J, Rowe T, Daniels M, Arnon TI, Gazit R, Joseph A, Schjetne KW, Steinle A, Porgador A, Mevorach D, Goldman-Wohl D, Yagel S, LaBarre MJ, Buckner JH, Mandelboim O. Novel APC-like properties of human NK cells directly regulate T cell activation. J Clin Invest 2004;114:1612–1623.
40. Colucci F, Caligiuri MA, Di Santo JP. What does it take to make a natural killer? Nat Rev Immunol 2003;3:413–425.
41. Pang G, Buret A, Batey RT, Chen QY, Couch L, Cripps A, Clancy R. Morphological, phenotypic and functional characteristics of a pure population of CD56+ CD16- CD3- large granular lymphocytes generated from human duodenal mucosa. Immunology 1993;79:498–505.
42. Leon F, Roldan E, Sanchez L, Camarero C, Bootello A, Roy G. Human small-intestinal epithelium contains functional natural killer lymphocytes. Gastroenterology 2003;125:345–356.
43. Lanier LL, Le AM, Civin CI, Loken MR, Phillips JH. The relationship of CD16 (Leu-11) and Leu-19 (NKH-1) antigen expression on human peripheral blood NK cells and cytotoxic T lymphocytes. J Immunol 1986;136:4480–4486.
44. Cooper MA, Fehniger TA, Turner SC, Chen KS, Ghaheri BA, Ghayur T, Carson WE, Caligiuri MA. Human natural killer cells: a unique innate immunoregulatory role for the CD56(bright) subset. Blood 2001;97:3146–3151.
45. Campbell JJ, Qin S, Unutmaz D, Soler D, Murphy KE, Hodge MR, Wu L, Butcher EC. Unique subpopulations of CD56+ NK and NK-T peripheral blood lymphocytes identified by chemokine receptor expression repertoire. J Immunol 2001;166:6477–6482.
46. Robertson MJ. Role of chemokines in the biology of natural killer cells. J Leukoc Biol 2002;71:173–183.
47. Podolsky DK. Inflammatory bowel disease. N Engl J Med 2002; 347:417–429.
48. Di Santo JP. Natural killer cell developmental pathways: a question of balance. Annu Rev Immunol 2006;24:257–286.
49. Spits H, Blom B, Jaleco AC, Weijer K, Verschuren MC, van Dongen JJ, Heemskerk MH, Res PC. Early stages in the development of human T, natural killer and thymic dendritic cells. Immunol Rev 1998;165:75–86.
50. Oida T, Suzuki K, Nanno M, Kanamori Y, Saito H, Kubota E, Kato S, Itoh M, Kaminogawa S, Ishikawa H. Role of gut cryptopatches in early extrathymic maturation of intestinal intraepithelial T cells. J Immunol 2000;164:3616–3626.
51. Mebius RE, Rennert P, Weissman IL. Developing lymph nodes collect CD4+CD3- LTbeta+ cells that can differentiate to APC, NK cells, and follicular cells but not T or B cells. Immunity 1997;7:493–504.
52. Yoshida H, Kawamoto H, Santee SM, Hashi H, Honda K, Nishikawa S, Ware CF, Katsura Y, Nishikawa SI. Expression of alpha(4)beta(7) integrin defines a distinct pathway of lymphoid progenitors committed to T cells, fetal intestinal lymphotoxin producer, NK, and dendritic cells. J Immunol 2001;167:2511–2521.
53. Fiocchi C, Tubbs RR, Youngman KR. Human intestinal mucosal mononuclear cells exhibit lymphokine-activated killer cell activity. Gastroenterology 1985;88:625–637.
54. Shibuya A, Nagayoshi K, Nakamura K, Nakauchi H. Lymphokine requirement for the generation of natural killer cells from CD34+ hematopoietic progenitor cells. Blood 1995;85:3538–3546.
55. Handgretinger R, Schafer HJ, Baur F, Frank D, Ottenlinger C, Buhring HJ, Niethammer D. Expression of an early myelopoietic antigen (CD33) on a subset of human umbilical cord blood-derived natural killer cells. Immunol Lett 1993;37:223–228.
56. Freud AG, Becknell B, Roychowdhury S, Mao HC, Ferketich AK, Nuovo GJ, Hughes TL, Marburger TB, Sung J, Baiocchi RA, Guimond M, Caligiuri MA. A human CD34(+) subset resides in lymph nodes and differentiates into CD56bright natural killer cells. Immunity 2005;22:295–304.
57. Keilbaugh SA, Shin ME, Banchereau RF, McVay LD, Boyko N, Artis D, Cebra JJ, Wu GD. Activation of RegIIIbeta/gamma and interferon gamma expression in the intestinal tract of SCID mice: an innate response to bacterial colonisation of the gut. Gut 2005;54:623–629.
58. Dalbeth N, Gundle R, Davies RJ, Lee YC, McMichael AJ, Callan MF. CD56bright NK cells are enriched at inflammatory sites and can engage with monocytes in a reciprocal program of activation. J Immunol 2004;173:6418–6426.
59. Yang L, Dybedal I, Bryder D, Nilsson L, Sitnicka E, Sasaki Y, Jacobsen SE. IFN-gamma negatively modulates self-renewal of repopulating human hemopoietic stem cells. J Immunol 2005; 174:752–757.

Received September 13, 2006. Accepted April 26, 2007.

Address requests for reprints to: Toshifumi Hibi, MD, PhD, Division of Gastroenterology and Hepatology, Department of Internal Medicine, School of Medicine, Keio University, 35 Shinano-machi Shinjuku-ku, Tokyo 160-8585, Japan. e-mail: thibi@sc.itc.keio.ac.jp; fax: (81) 3-3357-6156.

Supported in part by grants-in-aid from the Japanese Ministry of Education, Culture and Science, the Japanese Ministry of Health, Labor and Welfare, Keio University and Keio Medical Foundation, Tokyo, Japan.

The authors thank Professor Masaki Kitajima (Keio University, Japan), and Dr Tsuneo Fukushima (Yokohama Municipal Citizen's Hospital, Japan) for providing the specimens; Dr Atsushi Nakazawa, Dr Tomoharu Yajima, Dr Atsushi Sakuraba, and Mr Takaaki Nakai (Keio University) for critical discussion; and Professor Atsushi Saito, Dr Akira Hokama, and Dr Yoshimasa Yonamine (University of Ryukyus, Japan) for constructive advice.

Pathology International 2007; **57**: 413–420 doi:10.1111/j.1440-1827.2007.02117.x

Original Article

Blockade of interferon-γ-inducible protein-10 attenuates chronic experimental colitis by blocking cellular trafficking and protecting intestinal epithelial cells

Kenji Suzuki,[1] Yusuke Kawauchi,[1] Suresh S. Palaniyandi,[2] Punniyakoti T. Veeraveedu,[2] Masato Fujii,[3] Satoshi Yamagiwa,[1] Hiroyuki Yoneyama,[4] Gi Dong Han,[5,8] Hiroshi Kawachi,[5] Yoshiaki Okada,[6] Yoichi Ajioka,[7] Kenichi Watanabe,[2] Masamichi Hosono,[3] Hitoshi Asakura,[1] Yutaka Aoyagi[1] and Shosaku Narumi[4]

Departments of [1]Gastroenterology and Hepatology, [5]Cell Biology, Institute of Nephrology and [7]Pathology, Niigata University Graduate School of Medical and Dental Sciences, [2]Department of Clinical Pharmacology, Niigata University of Pharmacy and Applied Life Sciences, [3]Department of Life Science, Niigata University Graduate School of Science and Technology, Niigata City, [4]Stelic Institute and [6]Department of Bacterial and Blood Products, National Institute of Infectious Diseases, Tokyo, Japan and [8]Department of Food Science and Technology, Yeungnam University, Gyeongsan, Korea

The role of chemokines, especially CXCL10/interferon-γ-inducible protein 10 kDa (IP-10), a chemokine to attract CXCR3⁺ T-helper 1-type CD4⁺ T cells, is largely unknown in the pathophysiology of inflammatory bowel disease; ulcerative colitis and Crohn's disease. The authors have earlier shown that IP-10 neutralization protected mice from acute colitis by protecting crypt epithelial cells of the colon. To investigate the therapeutic effect of neutralization of IP-10 on chronic colitis, an anti-IP-10 antibody was injected into mice with newly established murine AIDS (MAIDS) colitis. Anti-IP-10 antibody treatment reduced the number of colon infiltrating cells when compared to those mice given a control antibody. The treatment made the length of the crypt of the colon greater than control antibody. The number of Ki67⁺ proliferating epithelial cells was increased by the anti-IP-10 antibody treatment. Terminal deoxynucleotidyl transferase-mediated dUTP nick-end labeling (TUNEL)⁺ apoptotic cells were observed in the epithelial cells of the luminal tops of crypts in control MAIDS colitis, whereas TUNEL⁺ apoptotic epithelial cells were rarely observed with anti-IP-10 antibody treatment. In conclusion, blockade of IP-10 attenuated MAIDS colitis through blocking cellular trafficking and protecting intestinal epithelial cells, suggesting that IP-10 plays a key role in the development of inflammatory bowel disease as well as in chronic experimental colitis.

Correspondence: Kenji Suzuki, MD, PhD, Department of Gastroenterology and Hepatology, Niigata University Graduate School of Medical and Dental Sciences, 1-757 Asahimachi-dori, Niigata 951-8510, Japan. Email: kjsuzuki@med.niigata-u.ac.jp

Received 3 October 2006. Accepted for publication 20 February 2007.

Key words: epithelial hyperplasia, IP-10, murine AIDS, ulcerative colitis

Chemokines, which are chemotactic cytokines, control the essential process of the attraction of leukocytes to tissues in inflammation.[1,2] The chemokine family consists of two major subfamilies, termed CXC and CC according to the arrangement of the first two conserved cysteines that are separated by one amino acid and are adjacent, respectively.[1,2] The interferon (IFN)-γ-inducible protein of 10 kDa (IP-10/CXCL10) is a member of the CXC chemokine family, and a potent chemoattractant for activated T lymphocytes, natural killer (NK) cells, and monocytes.[3,4] It is also considered as a regulator of the T-helper 1 (Th1) inflammatory response.[5] It has been reported that the expression of IP-10 was elevated in several diseases such as ulcerative colitis, hepatitis, multiple sclerosis, and Sjögren's syndrome, suggesting the involvement of IP-10 in the development of these diseases.[6–9] Information on the role of IP-10 in inflammatory bowel disease is limited, and needs further detailed investigation.

We have recently reported that neutralization of IP-10 protected mice from dextran sulfate sodium (DSS)-induced acute colitis by promoting crypt cell survival, without altering the infiltration of immune cells.[10] Furthermore, recombinant IP-10 administration into mice directly inhibited the intestinal epithelial cell proliferation.[10] In contrast, another report showed that IP-10 neutralization dominantly inhibited inflammation, and ameliorated colitis in interleukin-10 (IL-10)-deficient mice.[11] Thus, the therapeutic mechanism of IP-10 neutralization on experimental colitis has yet to be shown clearly.

The LP-BM5 murine leukemia virus (MuLV) is a retrovirus that induces profound immunodeficiency similar to that of human acquired immunodeficiency syndrome (AIDS), therefore it has been studied as a murine model of AIDS, thus termed murine AIDS (MAIDS).[12–15] We have previously reported that systemic exocrinopathy resembling Sjögren's syndrome and pancreatitis-like lesions were induced in mice with MAIDS, and colitis was not induced in MAIDS mice.[16,17] In contrast, nude mice inoculated with lymph node cells from mice with MAIDS developed chronic inflammatory bowel disease-like colitis, which we termed MAIDS colitis.[18] The precise mechanism of pathogenesis of the colitis remains largely unknown, however, regulatory T cells (Treg) deficiency might play a role in its development because there are some reports of colitis modulated by Treg.[19,20] We demonstrated that the pathological lesions of MAIDS colitis resembled ulcerative colitis, and that the major populations of colon-infiltrating cells in MAIDS colitis were $Mac1^+$ macrophages and $CD4^+$ T cells with polarized immune responses toward Th2.[21] Thus, MAIDS colitis could serve as an animal model for ulcerative colitis.

There have been other colitis models developed including DSS colitis, IL-10-deficient mice, and $Rag2^{-/-}$ mice reconstituted with $CD4^+CD45RB^{high}$ T cells, which are characterized as a Th1-dependent disease, mimicking Crohn's disease.[22] The diversity in the etiopathophysiology of these colitis models might induce different effects with IP-10 blockade. Therefore, to confirm the therapeutic mechanism of IP-10 neutralization, it is better to analyze the effect of anti-IP-10 treatment in different type of colitis models. In this report, to address this point, we investigated the effect of IP-10 neutralization on MAIDS colitis.

MATERIALS AND METHODS

Animals

Four-week-old female C57BL/6 (B6) mice were purchased from Charles River Japan (Atsugi, Japan). B6 nude mice were provided by Dr Norimitsu Satoh at the Animal Center of Niigata University School of Medicine. All mice were maintained at the same animal center under specific pathogen-free conditions. All animal experiments were performed according to the Guide for Animal Experimentation of Niigata University School of Medicine.

Induction of MAIDS and MAIDS colitis

Four-week-old B6 female mice were injected i.p. with 0.3 mL LP-BM5 MuLV stock solution. Induction of MAIDS was confirmed when the mice developed generalized lymphadenopathy. Eight weeks after virus inoculation, mice with MAIDS were killed by cervical dislocation under ether anesthesia, and their all lymph nodes were collected. To induce MAIDS colitis, the lymph nodes were pressed and passed through a steel mesh, and the cell suspension was transferred i.v. to 10–13-week-old female B6 nude mice at a dose of $3–5 \times 10^7$ lymph node cells/head. Symptoms of colitis such as diarrhea and anal bleeding were observed 3 weeks after cell transfer, and all the mice died within 6 weeks after cell transfer. LP-BM5 MuLV was prepared from the supernatant of cloned G6 cells infected with the retrovirus as reported previously.[16] For blocking experiments, PBS containing 100 μg/100 μL anti-CXCL10 mAb[10] or antihuman parathyroid-related peptide mAb, which was the IgG1 subclass-matched control mAb, or PBS alone were administered i.p. at the time of cell transfer and once a week thereafter. Three weeks after cell transfer, the mice were killed and their colons were removed for further analysis. Five mice were analyzed for each group and all the experiments were repeated three times.

Histopathological examination

Tissue samples were taken from the sigmoid colon, fixed in 10% buffered formalin, and then embedded in paraffin wax blocks. Four μm-thick sections were made in the usual way and stained with HE. The stained sections were then examined by light microscopy.

The entire colon (5 mice/group) was sampled. We analyzed the distal colon tissue section located approximately 10 mm from the anal verge to calculate the mean number of infiltrating cells of five different points in the lamina propria of the colon in a high-power field (×400) under a microscope. The crypt length of the colon of each mouse was also calculated as a mean value of five different crypts.

Preparation and flow cytometric analysis of cells that infiltrated the colon

Mouse colonic mucosal mononuclear cells were prepared as follows. Lamina propria mononuclear cells were isolated from the colon at 3 weeks after the induction of colitis as described here. Briefly, the entire colon was opened longitudinally, washed with PBS, and cut into small pieces. The pieces were then incubated with Ca^{2+}- and Mg^{2+}-free Hank's balanced salt solution (HBSS) containing 2.5% fetal bovine serum (FBS) and 1 mmol dithiothreitol (DTT) (Sigma-Aldrich, St Louis, MO, USA) for 30 min to remove mucus and then serially incubated twice in Ca^{2+}- and Mg^{2+}-free HBSS containing 2.5% FBS and 0.75 mmol EDTA (Sigma-Aldrich) for 1 h each. The supernatants from these incubations were collected, pooled, and treated with 1 mg/mL collagenase

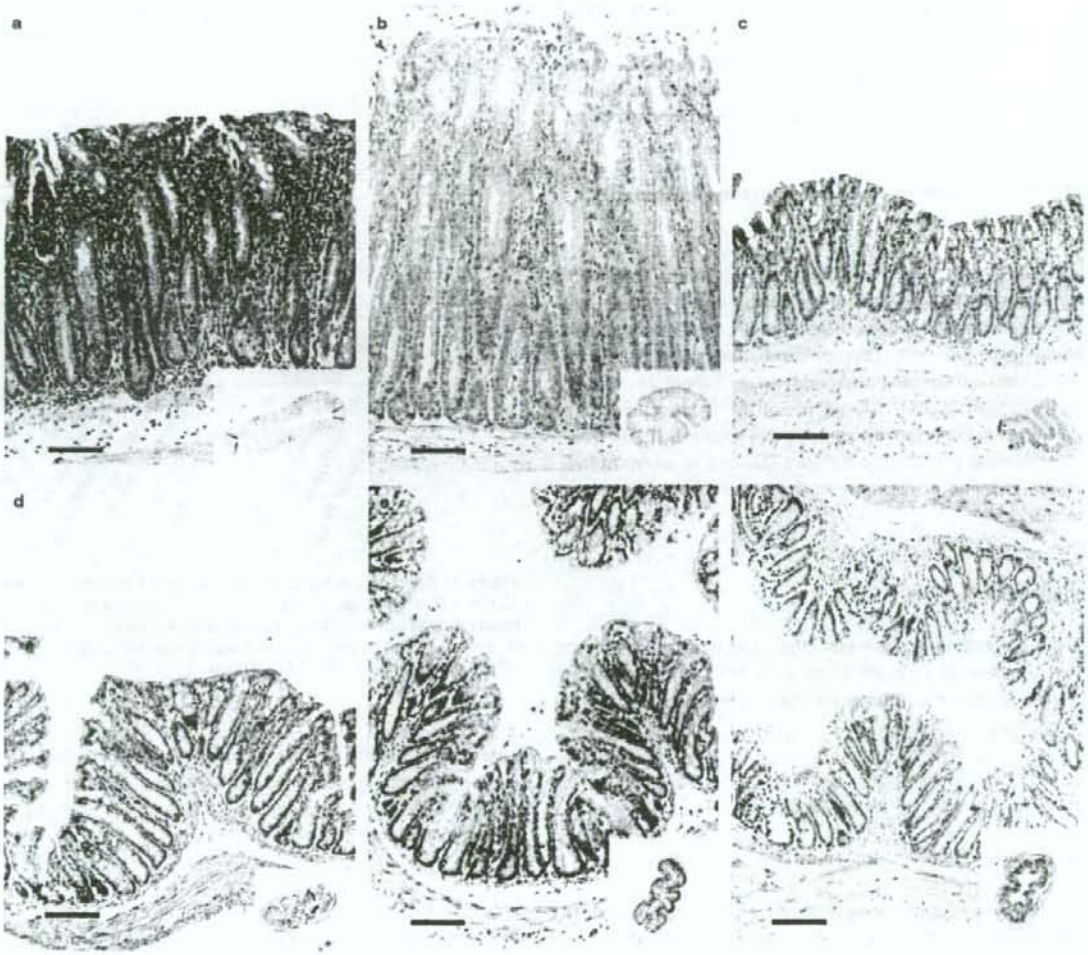

Figure 1 (a–d) Neutralization of interferon-γ-inducible protein 10 kDa (IP-10/CXCL10) attenuated murine acquired immunodeficiency syndrome (MAIDS) colitis. Distal colon tissues: (**a**) control antibody-treated mouse at 3 weeks after induction of colitis, (**b**) anti-IP-10 antibody-treated mouse, (**c**) normal B6 nude mouse, (**d**) normal B6 mouse, (**e**) anti-IP-10 antibody-treated B6 nude mouse, (**f**) anti-IP-10 antibody-treated B6 mouse. (**a**) Mild erosions of crypt epithelial cells at the tip of the crypt, and crypt abscess were observed in the MAIDS colitis. HE, original magnification ×100. Bars, 100 μm.

(Worthington Biomedical, Freehold, NJ, USA) and 0.01% Dnase (Worthington Biomedical) in medium for 2 h. The cells were pelleted twice through a 40% isotonic Percoll solution (Amersham Pharmacia Biotech AB, Uppsala, Sweden) and then further purified by Ficoll-Hypaque (Pharmacia, Inc., Pisataway, NJ, USA) density gradient centrifugation (40/75%) at 1300 *g*.

Cell suspensions were prepared in PBS containing 1% fetal calf serum and 0.1% sodium azide. The cells were incubated with anti-Fc receptor mAb (2.4G2) for 10 min at 4°C, and then incubated with fluorescent isothiocyanate (FITC)-conjugated mAb and phycoerythrin-conjugated mAb for 30 min. The stained cells were washed twice, resuspended, and analyzed using FACScan (Becton-Dickinson, Mountain View, CA, USA).

Immunohistochemical staining for Ki67

To evaluate the number of proliferating crypt epithelial cells of the colon, we used rabbit polyclonal anti-Ki67 antibody (YLEM, Rome, Italy). Formalin-fixed and paraffin-embedded

colon sections were deparaffinized with xylene and ethanol, and then incubated with the first antibody. FITC-labeled anti-rabbit sheep antibody was then reacted as a secondary antibody. The number of Ki67$^+$ crypt epithelial cells was evaluated under high-power fields on immunofluorescence microscopy.

Terminal deoxynucleotidyl transferase-mediated dUTP nick-end labeling

Apoptotic cells were identified using an *in situ* apoptosis-detection kit (Takara Biomedicals, Otsu, Japan) according to the manufacturer's instructions. In brief, paraffin-embedded colon sections were deparaffinized, rehydrated and then incubated with terminal deoxynucleotidyl transferase mixture containing FITC-dUTP for 90 min at 37°C. After mounting, terminal deoxynucleotidyl transferase-mediated dUTP nick-end labeling (TUNEL)$^+$ cells were counted in a crypt at five different points in high-power fields (×400) on fluorescent microscopy.

Statistical analysis

Data are expressed as mean ± SD. The unpaired Student's *t*-test or the non-parametric Mann–Whitney test was used for statistical analysis. Differences were considered significant at $P < 0.05$.

RESULTS

IP-10 neutralization attenuated MAIDS colitis

In mice treated with control antibody, a marked mononuclear cellular infiltration was observed in the mucosal and submucosal layer at 3 weeks after the induction of colitis (Fig. 1a) in comparison to normal B6 (Fig. 1c) or nude mice (Fig. 1d). Mild erosions of crypt epithelial cells were observed at the tip of crypt, and crypt abscess was also observed in some crypts (Fig. 1a). The number of infiltrating cells in the colon increased gradually with colon weight, and the crypt length significantly increased in MAIDS colitis with control antibody compared to untreated B6 or nude mice (Fig. 2). To evaluate the effect of IP-10 neutralization, we have analyzed the lesions of MAIDS colitis at 3 weeks after the induction of colitis (Fig. 1b). Because a long-term anti-IP-10 antibody treatment induced immunodeficiency and opportunistic infection such as pulmonary abscess at 6 weeks, we therefore carried out the analysis at 3 weeks after the induction of colitis. Neutralization of IP-10 decreased cellular infiltration into the colon of mice with MAIDS colitis (Fig. 2a). In addition, the length of the crypt became significantly greater by IP-10 blockade compared to control MAIDS colitis (Fig. 2b). Neutralization of IP-10 did not produce any significant change either in the number of cells in the lamina propria of the colon or in the length of the crypt of the colon in B6 nude or B6 mice (Figs 1e,f,2).

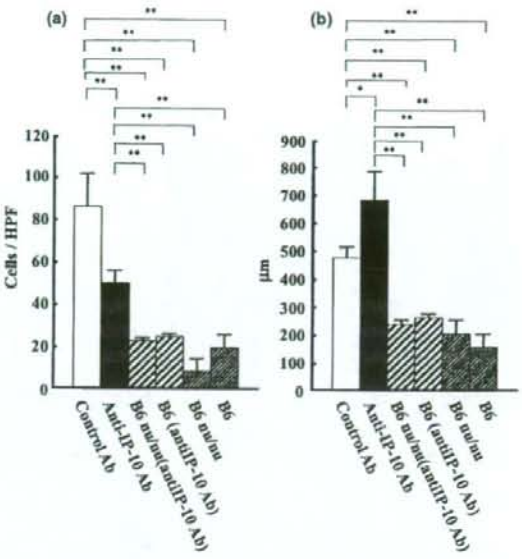

Figure 2 Effect of neutralization of interferon-γ-inducible protein 10 kDa (IP-10/CXCL10) on (**a**) number of infiltrating cells in the lamina propria of the colon at 3 weeks after induction of colitis and (**b**) crypt length of colon of mice at 3 weeks after induction of colitis. HPF, high-power field. $^*P < 0.05$; $^{**}P < 0.01$.

IP-10 neutralization reduced the number of immune cells in the colon of MAIDS colitis

Our previous immunohistochemical analyses showed that CD4$^+$ T cells and Mac1$^+$ macrophages are major populations in the colon of MAIDS colitis, with minor populations of CD8$^+$ T, and B cells.[18,21] In the present study, to determine the effect of IP-10 neutralization on the cellular components of the colon of MAIDS colitis, we analyzed the population of mucosal mononuclear cells that were isolated from the colon using a flow cytometer. In MAIDS colitis, CD4$^+$ and CD8$^+$ T cells with αβ T-cell receptors, and Mac1$^+$ cells were major populations that infiltrated the colon (Fig. 3). NK cells and granulocytes were minor populations (Fig. 3). Neutralization of IP-10 reduced the total number of inflammatory mononuclear cells infiltrating in the colon from 1.4×10^6 cells to 0.4×10^6 cells at 3 weeks after induction of the colitis. Additionally, IP-10 blockade significantly reduced the percentage

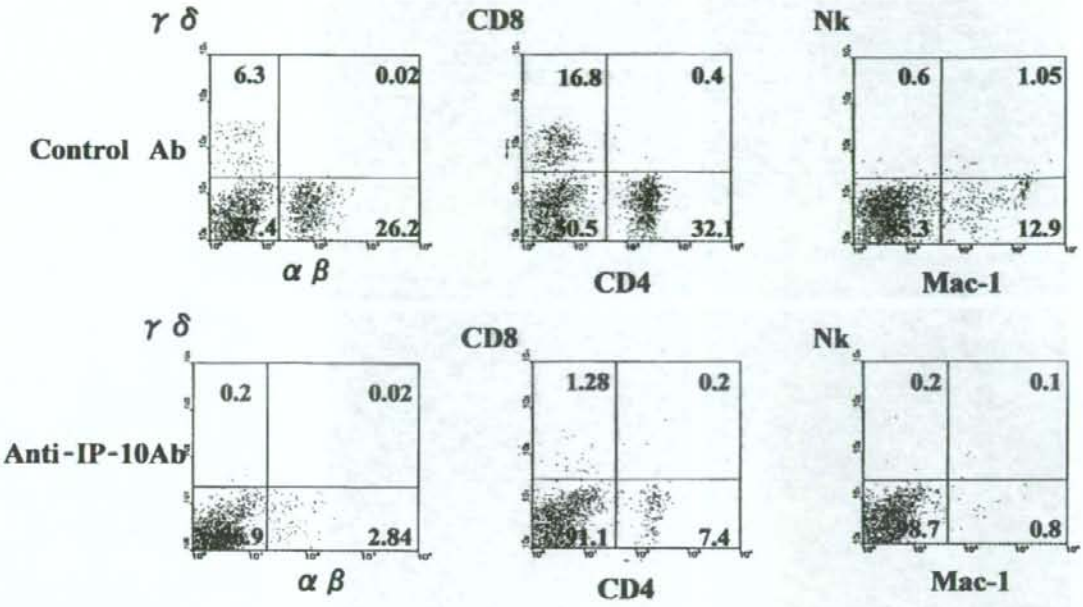

Figure 3 Neutralization of interferon-γ-inducible protein 10 kDa (IP-10/CXCL10) inhibited immune cell trafficking into the colon of murine acquired immunodeficiency syndrome (MAIDS) colitis. Two-color staining for T-cell receptor (TCR)-αβ and TCR-γδ, CD4 and CD8, and Mac1 and NK-1.1. Mononuclear cells in the colon of MAIDS mice at 3 weeks after induction of colitis were analyzed by flow cytometry; cells of mice treated with anti-IP-10 antibody were compared with those of mice treated with control antibody. Numbers in the figure represent the percentages of fluorescence-positive cells in corresponding areas. Representative results of three experiments are depicted.

of each population of $CD4^+$ and $CD8^+$ T cells possessing αβ T-cell receptors, and $Mac1^+$ cells in the colon (Fig. 3).

IP-10 neutralization increased $Ki67^+$ cells and decreased $TUNEL^+$ cells in the crypt epithelia of MAIDS colitis

We assessed the Ki67 staining to evaluate the proliferation effect of anti-IP-10 antibody treatment on colonic epithelial cells in attenuation of the colitis. In untreated B6 or B6 nude mice, $Ki67^+$ crypt epithelial cells were detected at basal one-fourth of a crypt (Fig. 4c–e). As we reported previously, crypt epithelial hyperplasia was observed in MAIDS colitis, and $Ki67^+$ cells were detected at one-third of the basal side of a crypt in the colon of MAIDS colitis with significantly increased number (Fig. 4a,e). Anti-IP-10 antibody treatment remarkably increased the number of $Ki67^+$ cells, and they were detected at a lower half of the crypt in anti-IP-10 mAb-treated mice (Fig. 4b,e).

Our previous report showed anti-apoptotic effect by IP-10 blockade on colonic epithelial cells in DSS colitis, therefore we assessed the apoptotic epithelial cells in the colons of mice with MAIDS colitis using the TUNEL method to detect DNA fragmentation *in situ*. $TUNEL^+$ apoptotic cells were observed in the epithelial cells of luminal tops of crypts in control MAIDS colitis (Fig. 5a). In anti-IP-10 antibody-treated mice, $TUNEL^+$ apoptotic epithelial cells were rarely observed (Fig. 5b).

DISCUSSION

In the present study we demonstrated that blockade of IP-10 attenuated MAIDS colitis not only by blocking cellular trafficking, but also by protecting crypt epithelial cells of the colon.

IP-10 was initially characterized as a chemoattractant for T lymphocytes, and binds to its receptor CXCR3, which is associated with Th1 immune responses.[1-4] The concept of selective mobilization of Th1 lymphocytes by IP-10 has been supported by several types of disease models[5] including multiple sclerosis,[23] rheumatoid arthritis, and inflammatory bowel disease.[11,24] Inflammatory bowel disease consists of two major forms: ulcerative colitis and Crohn's disease. Crohn's disease is suggested to be mediated by Th1-associated cytokines such as IL-23, IL-12, and IFN-γ that are overproduced by macrophages and T cells of lamina propria.

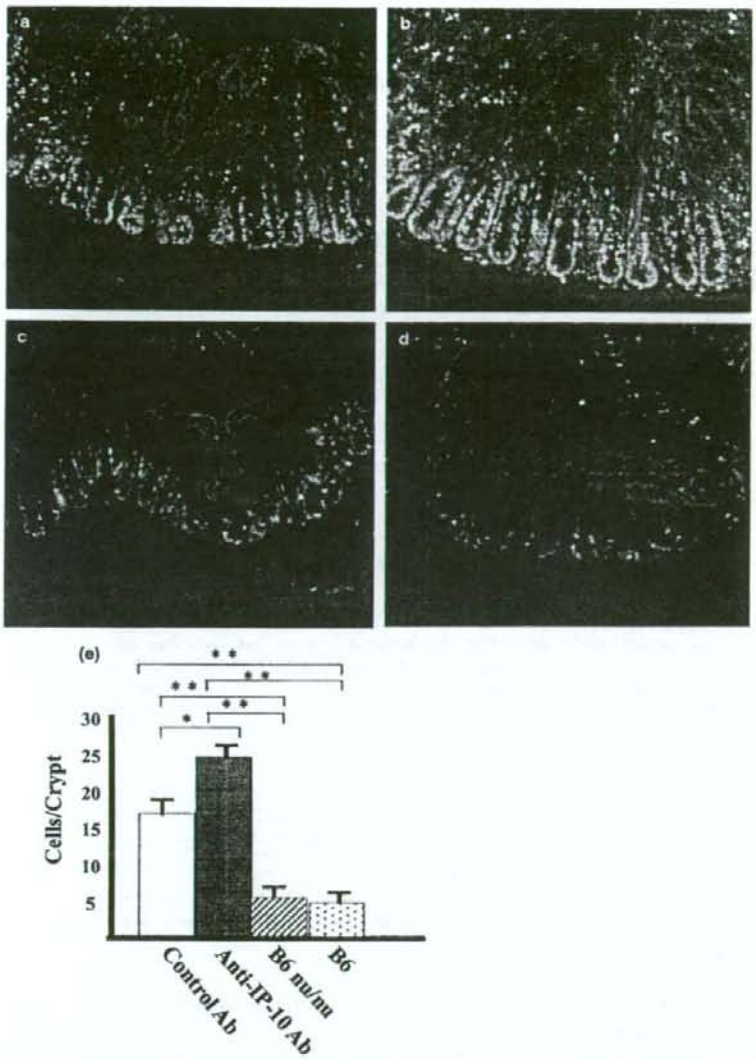

Figure 4 Neutralization of interferon-γ-inducible protein 10 kDa (IP-10/CXCL10) enhanced proliferation of crypt epithelial cells of the colon of murine acquired immunodeficiency syndrome (MAIDS) colitis. Ki67⁺ crypt epithelial cells were detected in (**a**) control antibody-treated MAIDS colitis mouse at 3 weeks after induction of colitis; (**b**) anti-IP-10 antibody-treated MAIDS colitis mouse; (**c**) normal B6 nude mouse; and (**d**) normal B6 mouse. (**e**) The number of Ki67⁺ crypt epithelial cells per crypt was increased in MAIDS colitis as compared with B6 and B6 nude mice. The number of cells was significantly increased by anti-IP-10 antibody treatment.

There have been developed many inflammatory bowel disease animal models. Among these, colitis observed in both IL-10-deficient mice and $Rag2^{-/-}$ mice reconstituted with $CD4^{+}CD45RB^{high}$ T cells has been characterized as a Th1-dependent disease, mimicking Crohn's disease.[22] Scheerens *et al.* have reported increased expression of mRNA of IP-10 in $Rag2^{-/-}$ mice reconstituted with $CD4^{+}CD45RB^{high}$ T cells, but not in IL-10-deficient mice.[24] Singh *et al.* showed that inhibition of IP-10 abrogates colitis in $IL\text{-}10^{-/-}$ mice supposedly by inhibiting the Th1 immune response.[11] They did not observe the hyperplasia of crypt epithelial cells of the colon induced by the blockade of IP-10 in the model. Thus, IP-10 neutralization is supposed to inhibit Th1 inflammatory reaction resulting in amelioration of colitis. To confirm the efficacy of the aforementioned mechanism, it is better to analyze the effect of anti-IP-10 treatment in different types of colitis models. We have established another experimental colitis model, that is, MAIDS colitis resembling ulcerative colitis.[18,21] In the present study, using this MAIDS colitis model, we also showed that IP-10 blockade significantly inhibited immune cell trafficking, leading to attenuation of the disease. Additionally we have recently reported that anti-IP-10 treatment ameliorates autoimmune-like pancreatic lesions in mice with MAIDS by blocking cellular trafficking.[25] Therefore, it is con-

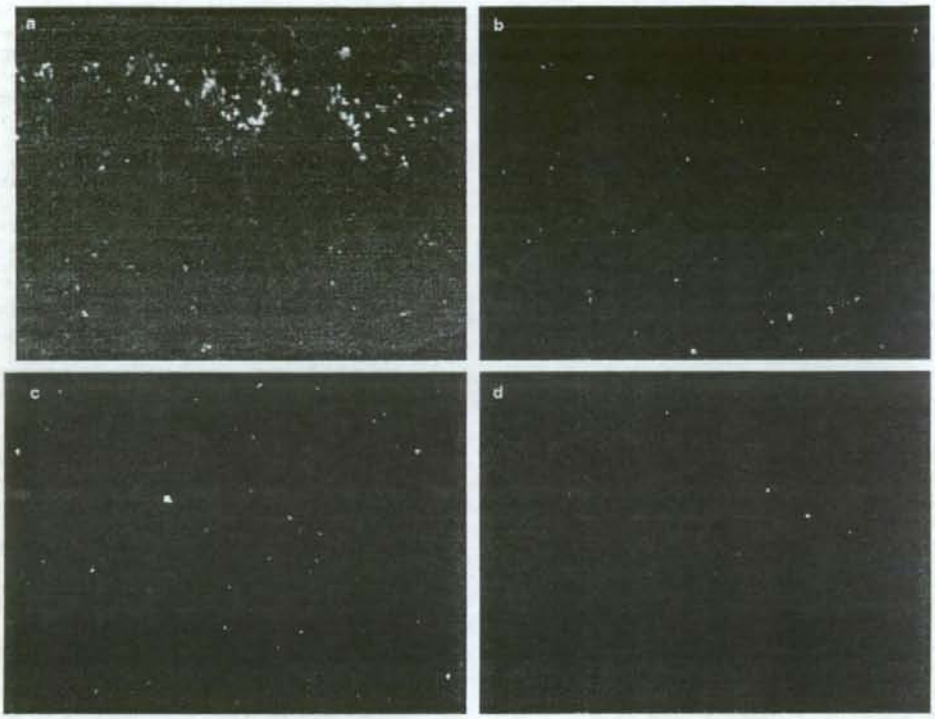

Figure 5 Anti-apoptotic death of crypt epithelial cells of colon by neutralization of interferon-γ-inducible protein 10 kDa (IP-10/CXCL10). (**a**) Terminal deoxynucleotidyl transferase-mediated dUTP nick-end labeling (TUNEL)$^+$ apoptotic cells were observed in the epithelial cells of luminal tops of crypts in murine acquired immunodeficiency syndrome (MAIDS) colitis; (**c**) TUNEL$^+$ apoptotic cells were rarely observed from B6 mice, (**d**) B6 nude mice and (**b**) mice treated with anti-IP-10 antibody.

ceivable that the main therapeutic effect of IP-10 neutralization in colitis, as well as in the other autoimmune diseases, is induced by inhibition of selective Th1 cells mobilization.

In our previous report we showed that neutralization of IP-10 protected mice from DSS-induced acute colitis by promoting crypt cell survival without altering immune cell infiltration.[10] Furthermore, recombinant IP-10 administration into normal mice directly inhibited intestinal crypt cell proliferation and migration *in vivo*.[10] Thus, we consider IP-10 a negative regulator of crypt cell proliferation and migration in the intestine. Initially DSS colitis was considered to be a T-cell-independent model because of the induction of colitis in T- and B-cell-lacking severe combined immunodeficient mice.[26] Later, however, both macrophage and T-cell responses were shown to play a pivotal role in the disease process, and the pathophysiology of DSS colitis is different from colitis observed in IL-10-deficient mice and Rag2$^{-/-}$ mice reconstituted with CD4$^+$CD45RB^{high} T cells.[22] This difference in pathophysiology of colitis might explain the different effect of IP-10 blockade on enhanced proliferation and anti-apoptosis of crypt epithelial cells or on inhibition of immune cell trafficking into the colon. As we have reported previously, both Th1 and Th2 immune responses were observed in MAIDS colitis, and hyperplasia of crypt epithelial cells is one of the characteristics of MAIDS colitis.[18,21] In the present study we demonstrated that IP-10 neutralization induced marked proliferation of crypt epithelial cells in MAIDS colitis as well as inhibition of immune cell trafficking. Neutralization of IP-10 did not show any change in the length of the crypt of the colon in B6 nude and B6 mice. In contrast, IP-10 neutralization for MAIDS colitis accelerated intestinal epithelial proliferation more significantly than untreated MAIDS colitis. These results suggest that IP-10 neutralization exerts its cell-proliferating effect more actively on the intestinal epithelial cells in inflammation, rather than on those in normal condition. We should analyze the synergistic relationship between IP-10 neutralization and cytokines and growth factors such as IFN-γ, IL-13, and IL-10, which are secreted by the immune cells recruited by IP-10, for the promotion of proliferation and anti-apoptosis of intestinal epithelial cells.

In conclusion, we have demonstrated that blockade of IP-10 ameliorated MAIDS colitis not only by blocking cellular trafficking, but also by facilitating the proliferation and anti-apoptosis of crypt epithelia of the colon. Neutralization of IP-10 could be a promising adjunctive therapy for inflammatory bowel disease.

ACKNOWLEDGMENTS

We thank Dr Xiu-Hua Yang and Mr Norio Honda for technical assistance. This work was supported by grants from the Ministry of Health, Welfare, and Labor of Japan.

REFERENCES

1 Luster AD. Chemokines: Chemotactic cytokines that mediate inflammation. *N Engl J Med* 1998; **338**: 436–45.
2 Baggiolini M. Chemokines and leukocyte traffic. *Nature* 1998; **392**: 565–8.
3 Luster AD, Ravetch JV. Biochemical characterization of a gamma interferon-inducible cytokine (IP-10). *J Exp Med* 1987; **166**: 1084–97.
4 Farber JM. Mig and IP-10: CXC chemokines that target lymphocytes. *J Leukoc Biol* 1997; **61**: 246–57.
5 Sallusto F, Lanzavecchia A, Mackay CR. Chemokines and chemokine receptors in T-cell priming and T helper 1/T helper 2-mediated responses. *Immunol Today* 1998; **19**: 568–74.
6 Uguccioni M, Gionchetti P, Robbiani DF *et al.* Increased expression of IP-10, IL-8, MCP-1, and MCP-3 in ulcerative colitis. *Am J Pathol* 1999; **155**: 331–6.
7 Narumi S, Tominaga Y, Tamaru M. Expression of IFN-inducible protein 10 in chronic hepatitis. *J Immunol* 1998; **158**: 5536–44.
8 Sorensen TL, Trebst C, Kivisakk P *et al.* Multiple sclerosis: A study of CXCL10 and CXCR3 co-localization in the inflamed central nervous system. *J Neuroimmunol* 2002; **127**: 59–68.
9 Ogawa N, Ping L, Zhenjun L, Takada Y, Sugai S. Involvement of the interferon-γ-induced T cell-attracting chemokines, interferon-γ-inducible 10-kd protein (CXCL10) and monokine induced by interferon-γ (CXCL9), in the salivary gland lesions of patients with Sjögren's syndrome. *Arthritis Rheum* 2002; **46**: 2730–41.
10 Sasaki S, Yoneyama H, Suzuki K *et al.* Blockade of CXCL10 protects mice from acute colitis and enhances crypt cell survival. *Eur J Immunol* 2002; **32**: 3197–205.
11 Singh UP, Singh S, Taub DD, Lillard JW Jr. Inhibition of IFN-γ-inducible protein-10 abrogates colitis in IL-10–/– mice. *J Immunol* 2003; **171**: 1401–6.
12 Mosier DE, Yetter RA, Morse HC III. Retroviral induction of acute lymphoproliferative disease and profound immunosuppression in adult C57BL/6 mice. *J Exp Med* 1985; **161**: 766–84.
13 Klinken SP, Fredrickson TN, Hartley JW. Evolution of B cell lineage lymphomas in mice with a retrovirus-induced immunodeficiency syndrome, MAIDS. *J Immunol* 1998; **140**: 1123–31.
14 Jolicoeur P. Murine acquired immunodeficiency syndrome (MAIDS): An animal model to study the AIDS pathogenesis. *FASEB J* 1991; **5**: 2398–405.
15 Cheung SC, Chattopadhyay SK, Hartley JW. Aberrant expression of cytokine genes in peritoneal macrophages from mice infected with LP-BM5 MuLV, a murine model of AIDS. *J Immunol* 1991; **146**: 121–7.
16 Suzuki K, Makino M, Okada Y *et al.* Exocrinopathy resembling Sjoegren's syndrome induced by a murine retrovirus. *Lab Invest* 1993; **69**: 430–35.
17 Watanabe S, Suzuki K, Kawauchi Y *et al.* Kinetic analysis of the development of pancreatic lesions in mice infected with a murine retrovirus. *Clin Immunol* 2003; **109**: 212–23.
18 Suzuki K, Narita T, Yui R *et al.* Induction of intestinal lesions in nu/nu mice induced by transfer of lymphocytes from syngeneic mice infected with murine retrovirus. *Gut* 1997; **41**: 221–8.
19 Izcue A, Coombes JL, Powrie F. Regulatory T cells suppress systemic and mucosal immune activation to control intestinal inflammation. *Immunol Rev* 2006; **212**: 256–71.
20 Fantini MC, Becker C, Tubbe I *et al.* Transforming growth factor beta induced FoxP3+ regulatory T cells suppress Th1 mediated experimental colitis. *Gut* 2006; **55**: 671–80.
21 Suriki H, Suzuki K, Baba Y *et al.* Analysis of cytokine production in the colon of nude mice with experimental colitis induced by adoptive transfer of immunocompetent cells from mice infected with a murine retrovirus. *Clin Immunol* 2000; **97**: 33–42.
22 Powrie F. T cells in inflammatory bowel disease: Protective and pathogenic role. *Immunity* 1995; **3**: 171–4.
23 Narumi S, Kaburaki T, Yoneyama H, Iwamura H, Kobayashi Y, Matsushima K. Neutralization of IFN-inducible protein10/CXCL10 exacerbates experimental autoimmune encephalomyelitis. *Eur J Immunol* 2002; **32**: 1784–91.
24 Scheerens H, Hessel E, De Waal-Malefyt R, Leach MW, Rennick D. Characterization of chemokines and chemokine receptors in two murine models of inflammatory bowel disease: IL-10$^{-/-}$ mice and Rag-2$^{-/-}$ mice reconstituted with CD4^{+}CD45RB^{high} T cells. *Eur J Immunol* 2001; **31**: 1465–74.
25 Kawauchi Y, Suzuki K, Watanabe S *et al.* Role of IFN-γ-inducible protein-10 (IP-10/CXCL10) in the progression of pancreatitis-like injury in mice after murine retroviral infection. *Am J Physiol Gastrointest Liver Physiol* 2006; **291**: G345–54.
26 Dieleman LA, Ridwan BU, Tennyson GS, Beagley KW, Bucy RP, Elson CO. Dextran sulfate sodium-induced colitis occurs in severe combined immunodeficient mice. *Gastroenterology* 1994; **107**: 1643–52.

Reciprocal Targeting of Hath1 and β-Catenin by Wnt Glycogen Synthase Kinase 3β in Human Colon Cancer

KIICHIRO TSUCHIYA, TETSUYA NAKAMURA, RYUICHI OKAMOTO, TAKANORI KANAI, and MAMORU WATANABE

Department of Gastroenterology and Hepatology, Graduate School, Tokyo Medical and Dental University, Tokyo, Japan

Background & Aims: **The transcription factor Hath1 plays a crucial role in the differentiation program of the human gut epithelium. The present study was conducted to investigate the molecular mechanism of Hath1 expression and its close association with β-catenin/glycogen synthase kinase 3β (GSK3β) under the Wnt pathway in human colonocytes.** ***Methods:*** **Tissue distribution of Hath1 messenger RNA in human tissues was examined by Northern blot. Stability of Hath1 protein was analyzed by expression of FLAG-tagged Hath1 in human cell lines. Targeting of Hath1 protein by GSK3β was determined by specific inhibition of GSK-3β function. Expression of Hath1 protein in colorectal cancers was examined by immunohistochemistry.** ***Results:*** **Hath1 messenger RNA expression was confined to the lower gastrointestinal tract in human adult tissues. In colon cancer cells, although Hath1 messenger RNA was also detected, Hath1 protein was positively degradated by proteasome-mediated proteolysis. Surprisingly, the GSK3β-dependent protein degradation was switched between Hath1 and β-catenin by Wnt signaling, leading to the dramatic alteration of cell status between proliferation and differentiation, respectively. Hath1 protein was detected exclusively in normal colon tissues but not in cancer tissues, where nuclear-localized β-catenin was present.** ***Conclusions:*** **The present study suggests a novel function of the canonical Wnt signaling in human colon cancer cells, regulating cell proliferation and differentiation by GSK3β-mediated, reciprocal degradation of β-catenin or Hath1, respectively, which further emphasizes the importance of aberrant Wnt signaling in colonocyte transformation.**

The gut epithelium undergoes continual renewal throughout adult life, maintaining the proper architecture and function of the intestinal crypts. This process involves highly coordinated regulation of the induction of cellular differentiation and the cessation of proliferation, and vice versa.[1–3] The intestinal epithelium consists of cells of 4 lineages: goblet cells, enteroendocrine cells, Paneth cells, and enterocytes.[4] Cellular differentiation into the former 3 lineages is believed to be regulated by a basic helix-loop-helix transcription factor called "Math1" in mice and "Hath1" in humans (officially termed as "ATOH1"). Math1 and Hath1 are known to play crucial roles in differentiation of various cells in other tissues, such as dorsal interneurons in the spinal cord,[5] granule cells in the cerebellum,[6] Merkel cells in the skin,[7] and inner hair cells in the auditory systems.[8]

In mice intestine, the *Math1* gene promotes the differentiation of epithelial cells to secretory lineage cells without affecting absorptive cell differentiation and is expressed in Ki-67–positive proliferating cells of the crypt, indicating a role of Math1 at an early stage of lineage commitment.[9] Expression of Math1 seems to be regulated at its transcriptional level, because forced expression of Notch intracellular domain in murine intestinal epithelial cells causes a decrease of Math1 messenger RNA (mRNA) expression and subsequent depletion of goblet cells in vivo.[10] Conversely, depletion of Hes1, another basic helix-loop-helix transcription factor known as a downstream target of Notch intracellular domain, up-regulates Math1 mRNA expression in murine intestine.[11] Thus, it is likely that *Math1* gene expression is regulated at the mRNA level by Notch signaling, leading to subsequent control of intestinal epithelial cell lineage decision of the crypt cells. It was recently reported that Hath1, a human homologue of Math1, up-regulates gastric mucin gene expression in gastric cells[12]; however, the regulation of Hath1 expression is less understood in human intestine.

The canonical Wnt signaling is another signaling pathway known to regulate cell differentiation and proliferation of the intestinal crypt cells.[13] It is believed that Wnt proteins induce inactivation of glycogen synthase kinase 3β (GSK3β), a component of the so-called destruction complex that also contains adenomatous polyposis coli (APC) and Axin, and the resultant dephosphorylation and stabilization of its substrate β-catenin leads to the transcription of genes targeted by the nuclear β-catenin/

Abbreviations used in this paper: APC, adenomatous polyposis coli; EGFP, enhanced green fluorescent protein; G3PDH, glyceraldehyde-3-phosphate dehydrogenase; GSK3β, glycogen synthase kinase 3b; RIPA, radioimmunoprecipitation assay; RT-PCR, reverse-transcription polymerase chain reaction; SDS, sodium dodecyl sulfate; siRNA, small interfering RNA; TCF, T-cell factor.

0016-5085/07/$32.00
doi:10.1053/j.gastro.2006.10.031

T-cell factor (TCF) complex.[14,15] However, in intestinal cells, it has not been shown whether activation of Wnt signaling simply inactivates general kinase activity of GSK3β or could possibly change the substrate specificity instead of kinase activity, thereby stabilizing the β-catenin protein. Constitutive activation of Wnt signaling is assumed to be essential for both continuous proliferation and maintenance of the undifferentiated state in intestinal stem cells.[16,17] Of note, the biological impact of the Wnt pathway lies in its close association with the carcinogenesis of colorectal cancer. Mutations that perturb the assembly or function of the destruction complex, such as truncation of APC, are present in approximately more than 90% of colorectal tumors. These mutations lead to constitutive activation of Wnt signaling, and the downstream genes that are transcriptionally up-regulated by the β-catenin/TCF complex are implicated in the growth-promoting properties of the tumor cells.[15,18] However, it has not been well understood how constitutive Wnt signaling could maintain colorectal cancer cells at an undifferentiated state.

A previous study reported that inhibition of Wnt signaling in a human colon cancer–derived cell line, HT-29, up-regulated both *Hath1* and *MUC2* gene mRNA expression.[19] This suggested that Hath1 expression may be suppressed at the mRNA level by the aberrant Wnt signaling, thereby maintaining the undifferentiated state of colorectal cancer cells. However, in the same study, it was also suggested that some colorectal cancers did express Hath1 mRNA at an amount comparable to the neighboring normal colon tissue but maintained an undifferentiated state at the same time.

These data prompted us to prove that *Hath1* gene function is regulated by the aberrant Wnt signaling, not only by the mRNA level but also by an unknown posttranscriptional or posttranslational mechanism in human colon cancer cells. Here, we present the evidence that Hath1 protein expression is regulated by Wnt signaling via GSK3β-mediated protein degradation. Our results suggest that the reciprocal regulation of Hath1 and β-catenin protein stability is mediated by GSK3β, which functions as a molecular switch regulating the proliferation and differentiation of colon cancer cells in vitro and in vivo. These results present a novel function of the Wnt-GSK3β pathway and further emphasize the importance of aberrant Wnt signaling in colonocyte transformation.

Materials and Methods

Cell Culture

Human colon cancer–derived SW480, DLD-1, and HT-29 cells and human embryonic kidney-derived 293T cells were grown in Dulbecco's modified Eagle medium (Life Technologies, Grand Island, NY) supplemented with 10% fetal bovine serum and 1% penicillin-streptomycin. In all experiments, 1×10^6 cells were seeded onto 6-cm culture dishes 36 hours before the experiment. All transfection experiments of DNA constructs and small interfering RNA (siRNA) oligonucleotides were performed by using TransIT transfection reagent (Mirus, Madison, WI) according to the manufacturer's instructions.

DNA Constructs

pcDNA3-Myc-ubiquitin[20] was a kind gift from Dr K. Tanaka (Tokyo Metropolitan Institute, Tokyo, Japan). pMX-IRES-GFP[21] was a kind gift from Dr T. Kitamura (University of Tokyo, Tokyo, Japan). Series of expression vectors encoding mutants for *APC* genes (pCS2-APC2, -APC3, and -APC25)[22] and a pRL5-Wnt1[23] were kind gifts from Dr H Shibuya (Tokyo Medical and Dental University, Tokyo, Japan). Expression plasmids encoding N-terminally Flag-tagged WT-Hath1 (pCMV-Flag-WT-Hath1) or enhanced green fluorescent protein (EGFP) (pCMV-Flag-EGFP) were generated by inserting the polymerase chain reaction (PCR)-amplified *Hath1* gene or *EGFP* gene, respectively, into the *Eco*RI/*Bam*HI site of a pCMV-Flag vector (Stratagene, La Jolla, CA) in frame. Plasmids for various mutants that lack either the N- or C-terminal region of Hath1 (N1-5, C1, and C2 mutants; Figure 3*A*) and the mutant 54/58SA-Hath1, in which both 54S and 58S are substituted to alanines, were constructed by PCR-mediated mutagenesis by using pCMV-Flag-WT-Hath1 as a starting material. pMX-Flag-WT-Hath1-IRES-GFP was generated by inserting a fragment encoding the N-terminally Flag-tagged *Hath1* gene, which was amplified by PCR using pCMV-Flag-WT-Hath1 as a template, into the pMX-IRES-GFP vector. A reporter plasmid E-box Luc was generated by inserting a 77–base pair oligonucleotide containing 7 repeats of the E-box (kE sites) (AGGCAGGTGGC) into an *Sma*I site of the pTA-Luc vector (Clontech, Mountain View, CA). Reporter plasmids TOPflash and FOPflash were obtained from Upstate Biotechnology (Charlottesville, VA). All plasmids constructed were verified by sequencing.

Immunoblottings and Immunoprecipitations

Cells were transfected with 1 μg of pCMV-Flag vector (control), pCMV-Flag-EGFP, pCMV-Flag-Hath1, or various mutants of pCMV-Flag-Hath1. In cotransfection experiments, 1 μg of either pcDNA3-Myc-ubiquitin or one of the expression plasmids for mutant APC (pCS2-APC2, -APC25, or -APC3) or pRL5-Wnt1 was transfected along with 1 μg of pCMV-Flag vector (control) or pCMV-Flag-Hath1. In each cotransfection experiment, the total amount of DNA was equalized by adding the appropriate amount of empty expression vector. After 12 hours of transfection, cells were cultured for 12 hours under the usual conditions or in the presence of 10 μmol/L lactacystin (Calbiochem, San Diego, CA), 10 μmol/L MG132 (Calbiochem), 5 μmol/L calpain inhibitor (Calbiochem),

100 μmol/L chloroquine (Sigma-Aldrich, St Louis, MO), 100 μmol/L RO-31-8220 (Calbiochem), 100 μmol/L staurosporine (Calbiochem), 1 μmol/L UO126 (Calbiochem), 30 mmol/L LiCl (Sigma-Aldrich), 30 mmol/L kenpaullone (Calbiochem), or 5 μmol/L BIO (Calbiochem).

For siRNA experiments, SW480 cells were transfected with 100 nmol/L siRNA oligonucleotide along with 1 μg of pCMV-Flag-WT-Hath1 for 12 hours, cultured for an additional 12 hours under the usual conditions, and then treated with MG132 or left untreated for 12 hours. A siRNA oligonucleotide specific for human GSK3β was obtained from Santa Cruz Biotechnology (Santa Cruz, CA), and a negative control (nonsense siRNA) oligonucleotide was synthesized as described elsewhere.[24] After transfection, cells were harvested, washed with phosphate-buffered saline (PBS) once, and incubated on ice for 15 minutes in 1% sodium dodecyl sulfate (SDS)-containing radioimmunoprecipitation assay (RIPA) buffer (10 mM Tris-HCl [pH 8.0], 1% Triton X-100, 1% SDS, 0.1% sodium deoxycholate, 1 mmol/L EDTA, 0.5 mmol/L ethylene glycol-bis(β-aminoethyl ether)-*N,N,N',N'*-tetraacetic acid, and 140 mmol/L NaCl). After brief sonication of the lysates to shear genomic DNA, the samples were centrifuged for 20 minutes and the supernatant was used as whole cell extract. The protein concentration in each sample was determined by using protein assay reagent (Pierce, Rockford, IL). For immunoblotting, 50 μg or 100 μg of whole cell extract was separated in 12% SDS-polyacrylamide gels, transferred to polyvinylidene difluoride membranes, blocked, and probed according to standard procedures.[24] The following antibodies and dilutions were used: mouse anti-Flag M2 (Sigma Chemical Co, St Louis, MO), 1:5000; mouse anti-dephospho-β-catenin (Alexis, San Diego, CA), 1:500; mouse anti-GSK3 (Calbiochem), 1:1000; rabbit anti-USF2 (loading control for the amount of nuclear proteins; Santa Cruz Biotechnology), 1:1000; and mouse anti-β-actin (loading control for the whole cell extracts; Sigma Chemical Co), 1:5000. Horseradish peroxidase-conjugated secondary antibodies were used for mouse (Amersham Biosciences UK, Buckinghamshire, England) and rabbit immunoglobulin G (Cell Signaling Technology, Danvers, MA). Blots were visualized with the ECL Plus System (Amersham Biosciences UK) by using a Lumi-Imager F1 system (Roche Diagnostics, Rotkreutz, Switzerland). For immunoprecipitation assays, 300 μg of whole cell extract in 1% SDS-containing RIPA buffer was diluted with 9 vol of non-SDS-containing RIPA buffer to give an SDS concentration of 0.1%, and then the total volume was adjusted to 1 mL by adding an appropriate amount of 0.1% SDS-containing RIPA buffer. The lysates were precleared by incubation with 40 μL of protein G/Sepharose (50% slurry in 0.1% SDS-RIPA buffer) for 1 hour, and then the supernatants were incubated with 1 μg of anti-Flag M2 antibody (Sigma Chemical Co) overnight. A 40-μL aliquot of 50% protein G/Sepharose slurry was added to each sample and incubated for 2 hours at 4°C. Precipitates were washed 3 times in 0.1% SDS-containing RIPA buffer, resolved by SDS/polyacrylamide gel electrophoresis, and analyzed by immunoblotting using a mouse anti-myc antibody (Invitrogen, Carlsbad, CA) at 1:1000 dilution. Protein visualization was performed as described previously.

Semiquantitative Reverse-Transcription PCR and Northern Blotting

Total RNA was isolated by using TRIzol reagent (Invitrogen). Aliquots of 5 μg of total RNA were used for complementary DNA synthesis in 21 μL of reaction volume by using oligo dT primers. One microliter of complementary DNA was amplified with 0.25 U of LA Taq polymerase (Takara Bio, Otsu, Japan) in a 25-μL reaction. Sense and antisense primers and the cycle numbers for the amplification of each gene were as follows: sense Flag, 5′-CACCATGGATTACAAGGATGACGACGAT-3′ and antisense Hath1, 5′-TTGCCCGCGCCCCCTTCATAG-3′ for the fragment covering the region for Flag-Hath1 (20 cycles); sense Flag, 5′-CACCATGGATTACAAGGATGACGACGAT-3′ (common for the S primer for the Flag-Hath1 fragment) and antisense Flag-EGFP, 5′-AGGATGTTGCCGTCCTCC-3′ for Flag-EGFP (20 cycles); sense GSK3β, 5′-ATCTTAATCTGGTGCTGGACTATGT-3′ and antisense GSK3β, 5′-TTGAGTGGTGAAGTTGAAGAGTGCA-3′ for GSK3β (25 cycles); sense MUC2, 5′-CTGCACCAAGACCGTCCTCATG-3′ and antisense MUC2, 5′-GCAAGGACTGAACAAAGACTCAGAC-3′ for MUC2 (25 cycles); sense c-Myc, 5′-CTTCTGCTGGAGGCCACAGCAAACCTCCTC-3′ and antisense-c-Myc, 5′-CCAACTCCGGGATCTGGTCACGCAGGG -3′ for c-Myc (25 cycles); sense Hath1, 5′-AAGACGTTGCAGAAGAGACCCG-3′ and antisense Hath1, 5′- TTGCCCGCGCCCCCTTCATAG-3′ (common for the antisense primer for Flag-Hath1 fragment) for endogenous Hath1 (25 cycles); and sense glyceraldehyde-3-phosphate dehydrogenase (G3PDH), 5′-TGAAGGTCGGAGTCAACGGATTTGGT-3′ and antisense G3PDH, 5′-CATGTGGGCCATGAGGTCCACCAC-3′ for glyceraldehyde-3-phosphate dehydrogenase (17 cycles). The amplification for each gene was logarithmic under these conditions. PCR products were separated on 1.5% agarose gels, stained with ethidium bromide, and visualized with a Lumi-Imager F1 (Roche Diagnostics).

Expression levels of Hath1 mRNA in human tissues were analyzed by using 2 human multiple tissue blots (BioChain Institute, Hayward, CA). The complementary DNA probe corresponding to nucleotides +1/+749 for the *Hath1* gene was generated by reverse-transcription (RT)-PCR from an RNA sample obtained from human colonic tissues. The probe for G3PDH was also generated by RT-PCR. The probes were labeled with [α-32P]deoxycytidine triphosphate by random priming using RediPrime II (Amersham Biosciences UK) according to the